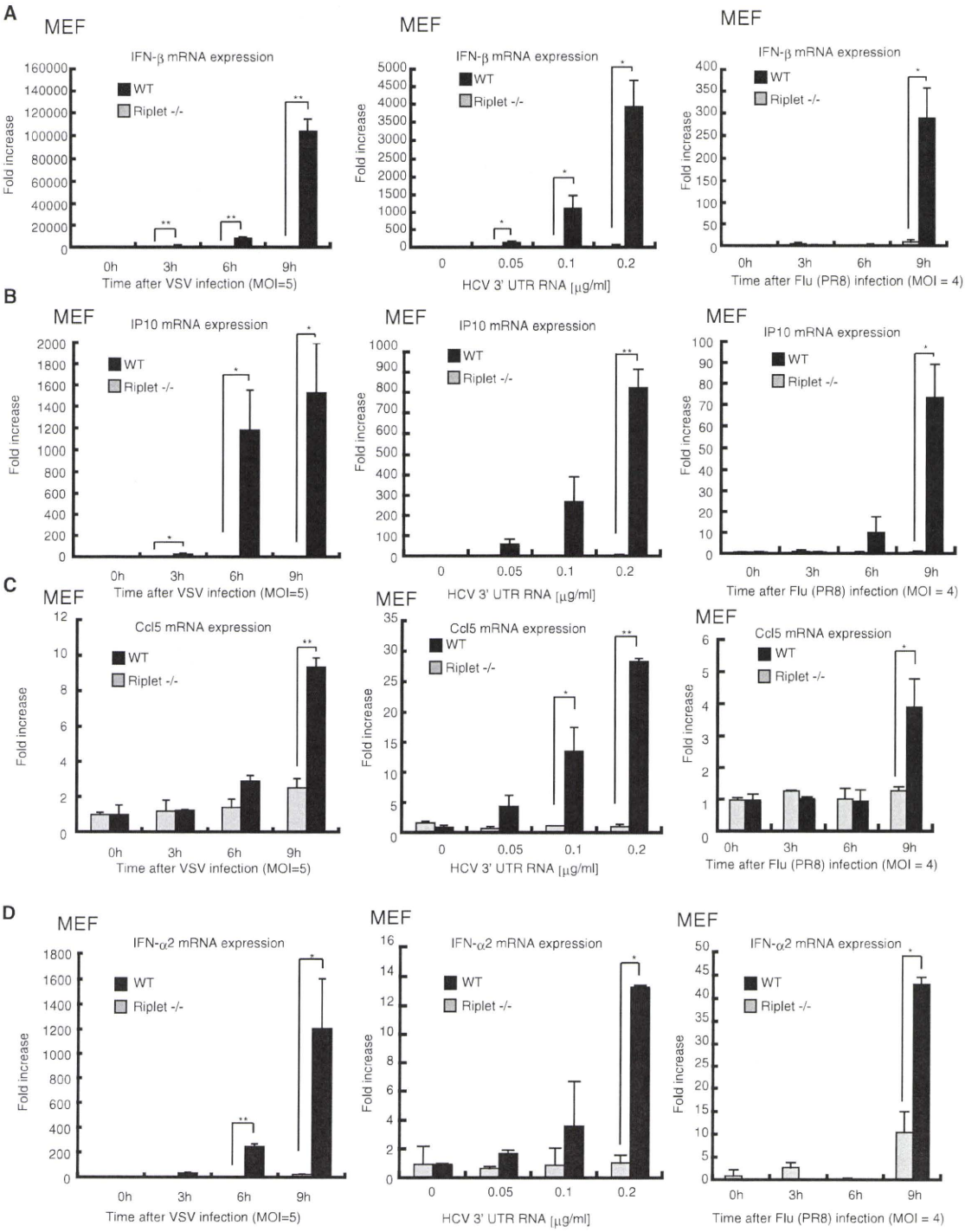

Figure 2. Abolished Responses to RNA Virus Infection in *Riplet*$^{-/-}$ Fibroblasts

Wild-type or *Riplet*$^{-/-}$ MEFs were infected with VSV or influenza A virus (Flu), and total RNA was extracted at the indicated times. Short HCV 3′UTR dsRNA was transfected into wild-type or *Riplet*$^{-/-}$ MEFs, and total RNA was extracted after 24 hr. Extracted RNA was subjected to RT-qPCR to determine IFN-β (A), IP10 (B), Ccl5 (C), or IFN-α2 (D) expression. Expression of each sample was normalized to β-actin mRNA expression. Data are shown as means ±SD and are representative of three independent experiments. *$p < 0.05$, **$p < 0.01$ (t test).

See also Figure S2 and Table S1.

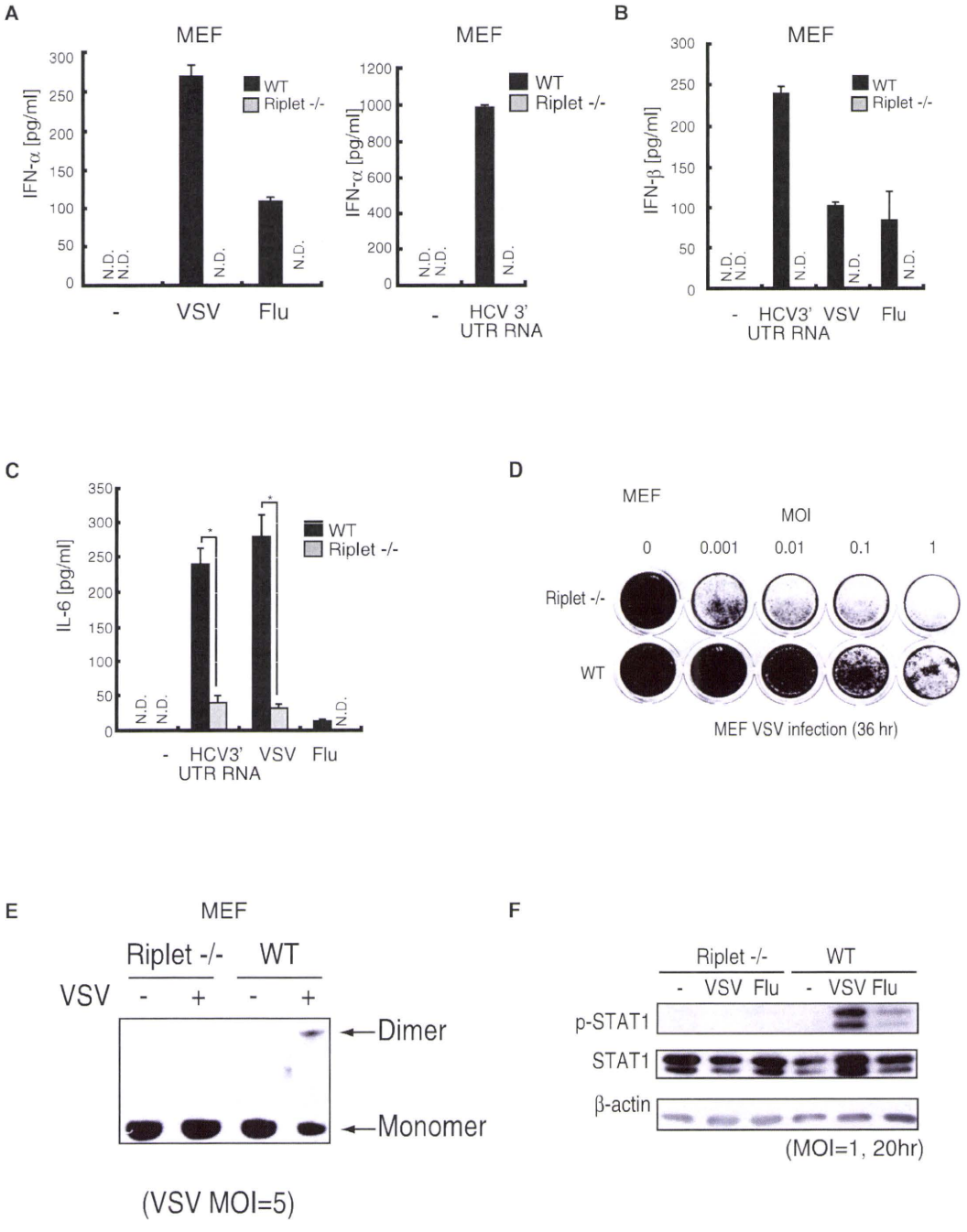

Figure 3. Role of Riplet in Antiviral Responses in Fibroblasts

(A–C) Wild-type or *Riplet*$^{-/-}$ MEFs were infected with VSV or Flu or transfected with short HCV 3′UTR dsRNA. Amounts of IFN-α (A), -β (B), and IL-6 (C) in culture supernatants were measured by ELISA after 24 hr. Data are shown as means ±SD and are representative of three independent experiments. *$p < 0.05$, **$p < 0.01$ (t test).

(D) Wild-type or *Riplet*$^{-/-}$ MEFs were infected with VSV at the indicated moi, and after 36 hr MEFs were fixed with formaldehyde and stained with crystal violet.

(E) Wild-type or *Riplet*$^{-/-}$ MEFs were infected with VSV at moi = 5, and after 9 hr cell lysates were prepared and analyzed by native PAGE. IRF-3 proteins were stained with anti-IRF3 antibody.

(F) Wild-type or *Riplet*$^{-/-}$ MEFs were infected with VSV or Flu at moi = 1, and after 20 hr cell lysates were prepared. The samples were analyzed by SDS-PAGE and western blotting. They were stained with anti-STAT1, phospho-STAT1, or β-actin antibodies.

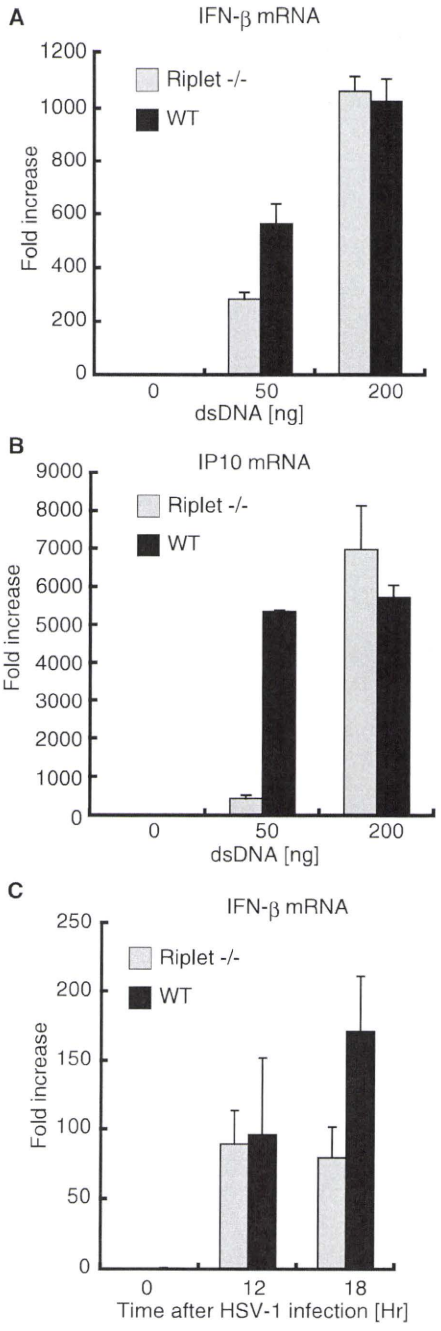

Figure 4. Role of Riplet in Type I IFN Production Induced by Cytoplasmic dsDNA

(A and B) Wild-type and *Riplet*$^{-/-}$ MEFs were transfected with the indicated amounts of dsDNA (Salomon sperm DNA) using the Lipofectamine 2000 reagent. Nine hours after the transfection, IFN-β (A) and IP-10 (B) mRNA expression was determined by RT-qPCR. Data are shown as means ±SD and are representative of three independent experiments.

(C) Wild-type and *Riplet*$^{-/-}$ MEFs were infected with HSV-1 at moi = 4, and IFN-β mRNA expression at the indicated times was examined by RT-qPCR. Data are shown as means ±SD and are representative of three independent experiments.

6A–6F). Similar to cDCs, cytokine production was reduced in Riplet knockout mice (Figures 6A–6F). Peritoneal Mf were isolated from wild-type and *Riplet*$^{-/-}$ mice. Knockout of Riplet reduced type I IFN production from peritoneal Mfs during VSV infection (Figures S4C and S4D).

We next generated Flt3L-induced DCs (Flt3L-DCs), which contain pDCs. Akira and his colleagues previously showed that the knockout of RIG-I or IPS-1 does not reduce type I IFN and IL-6 production by Flt3L-DCs, because RIG-I is dispensable for cytokine production in pDCs (Kato et al., 2005). The Flt3L-DCs of *Riplet*$^{-/-}$ mice produced normal amounts of IFN-a, -β, and IL-6 during Flu infection (Figures 6A–6F). This is consistent with the notion that Riplet is essential for the RIG-I-mediated type I IFNs and IL-6 production. Although the IFN-α levels in the culture medium after VSV infection were comparable with those in wild-type and *Riplet*$^{-/-}$ mice, Flt3L-DCs of *Riplet*$^{-/-}$ mice produced less IL-6 compared with that produced by wild-type mice through an unknown mechanism (Figure 6C).

Next, we examined type I IFN production during SeV infection. SeV infection induced IFN-α and -β productions from wild-type BM-DC, and the knockout of Riplet reduced IFN-α and -β productions from BM-DC (Figures S4E–S4J). Wild-type Flt3L-DC produced IFN-α after SeV infection, and the knockout of Riplet did not reduce IFN- α production from Flt3L-DC (Figures S4E–S4J).

Riplet Is Essential for Antiviral Immune Defense In Vivo

To investigate the role of Riplet in antiviral responses in vivo, wild-type and *Riplet*$^{-/-}$ mice were injected intraperitoneally with wild-type VSV, and sera were collected to measure type I IFN and IL-6 levels. IFN-α, -β, and IL-6 levels in sera were markedly reduced in *Riplet*$^{-/-}$ mice compared to in wild-type mice (Figures 7A and 7B, and Figure S5A). Next, wild-type and *Riplet*$^{-/-}$ mice were intranasally infected with VSV, and type I IFN levels in their sera were measured. At early time points, IFN-α and -β production was reduced in *Riplet*$^{-/-}$ mice compared to wild-type mice (Figures 7C and 7D); however, cytokine levels were comparable at later time points (Figures S5B and S5C). Previously, Ishikawa et al. observed that the knockout of STING gene, which is involved in RIG-I-dependent signaling, leads to reduction of type I IFN at early time points and relatively less reduction at later time points (Ishikawa and Barber, 2008; Ishikawa et al., 2009).

To determine if Riplet deficiency affects the survival of mice after VSV infection, the mice were intranasally infected with VSV, and their survival was monitored. Wild-type mice survived VSV infection; however, *Riplet*$^{-/-}$ mice were susceptible to VSV infection (Figure 7E). The viral titer in *Riplet*$^{-/-}$ mice brains 7 days after infection was higher than in wild-type mice (Figure 7F). These data indicate that Riplet plays a key role in the host defenses against VSV infection in vivo, and type I IFN production at early time points is important for host defenses.

DISCUSSION

In this study, we presented genetic evidence that Riplet is indispensable for antiviral responses in MEFs, BM-Mf, and BM-DCs, but not in Flt3L-DCs. The cell-type-specific requirement of Riplet

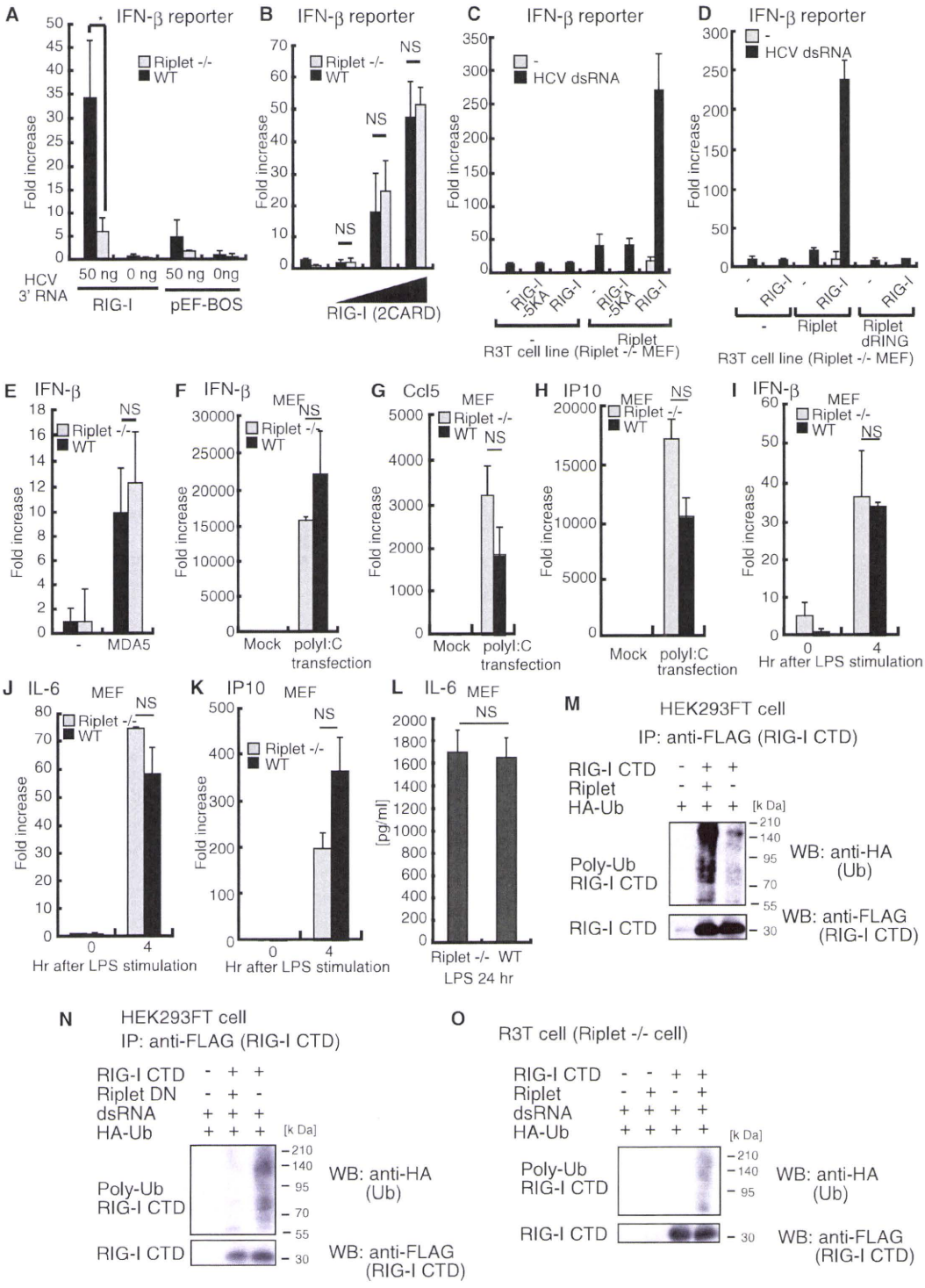

Figure 5. Role of Riplet in the RIG-I-Dependent Pathway

(A) Expression vector of full-length RIG-I and reporter plasmids were transfected into wild-type or *Riplet*$^{-/-}$ MEFs with or without HCV 3′UTR short dsRNA, and after 24 hr IFN-β promoter activation was examined by reporter gene assay. Data are shown as means ±SD and are representative of three independent experiments. *$p < 0.05$ (t test).

is similar to that of RIG-I. Previously, we showed that Riplet binds to RIG-I and mediates Lys63-linked polyubiquitination of RIG-I (Oshiumi et al., 2009). Genetic evidence in this study revealed that Riplet function is essential for RIG-I-dependent type I IFN production. Knockout of Riplet reduced type I IFN production in vivo during the early phase of VSV infection, and *Riplet*$^{-/-}$ mice were susceptible to VSV infection. Taken together, our results provide genetic evidence that Riplet is essential for RIG-I-dependent antiviral immune response in vivo. Most *RIG-I*$^{-/-}$ embryos were lethal at embryonic days 12.5–14.0 in some strain backgrounds (Kato et al., 2005). However, we could not observe any developmental defect in Riplet knockout mice as far as we examined.

Previously, Chen and his colleagues independently isolated Riplet and named it REUL (Gao et al., 2009). They reported that REUL/Riplet binds to RIG-I CARDs but not to CTD (Gao et al., 2009). Furthermore, they reported that REUL/Riplet mediates Lys63-linked polyubiquitination of Lys172 of RIG-I CARDs in a manner similar to TRIM25 (Gack et al., 2007; Gao et al., 2009). Although they did not show any expression profile data for Riplet and TRIM25, they mentioned that TRIM25 and Riplet have different distribution patterns, and thus hypothesized that REUL/Riplet is a complementary factor of TRIM25 and is required for RIG-I activation in cells that do not express TRIM25 (Gao et al., 2009). However, our genetic evidence is not consistent with their hypothesis, because Riplet is essential for RIG-I activation in MEFs that express TRIM25. Previously, Gack et al. showed that knockout of TRIM25 alone abolished RIG-I activation in MEFs (Gack et al., 2007). Therefore, null mutation in either Riplet or TRIM25 abolishes RIG-I activation. This genetic evidence indicates that Riplet can mediate polyubiquitination of RIG-I Lys residues that are not ubiquitinated by TRIM25. This means that Riplet functions differently than TRIM25 in RIG-I activation.

We isolated Riplet cDNA by yeast two-hybrid screening using the C-terminal region of RIG-I (Oshiumi et al., 2009). Because the yeast genome does not encode RIG-I, the interaction indicates the direct binding of Riplet to the RIG-I C-terminal region. The interaction between RIG-I CTD and Riplet has also been confirmed by immunoprecipitation assays in human cells (Oshiumi et al., 2009). Moreover, we have shown that Riplet expression leads to Lys63-linked polyubiquitination of RIG-I CTD (Oshiumi et al., 2009). Recently, Zheng et al. showed that RIG-I CARDs has the ability to bind to polyubiquitin chains (Zeng et al., 2010). We have carefully detected Riplet-mediated polyubiquitination of RIG-I C-terminal region without CARDs, under high-salt conditions, in which many protein-protein interactions were abolished (Oshiumi et al., 2009). Therefore, we proposed the hypothesis that Riplet mediates Lys63-linked polyubiquitination of RIG-I CTD (Oshiumi et al., 2009). This model can explain the genetic evidence that Riplet is essential for RIG-I activation in MEFs that express TRIM25. Gack et al. showed that K172R mutation alone caused near-complete loss of ubiquitination of the human RIG-I CARDs (Gack et al., 2007). Because residue 172 of mouse RIG-I is not Lys but Gln (Shigemoto et al., 2009), Riplet/Reul does not ubiquitinate residue 172 of mouse RIG-I. Based on the previous studies and our current data, we prefer the interpretation that Riplet activates RIG-I through polyubiquitination of RIG-I CTD. However, this interpretation does not exclude the possibility that Riplet ubiquitinates both CTD and CARDs of RIG-I (Gao et al., 2009; Oshiumi et al., 2009).

Previously, we showed that Lys849, -851, -888, -907, and -909 are critical residues in Riplet-mediated RIG-I CTD ubiquitination (Oshiumi et al., 2009). These five Lys residuse are close to the dsRNA binding sites of RIG-I CTD (Takahasi et al., 2008), and the 5KA mutation weakly reduced RNA binding activity of RIG-I. Therefore, it is possible that the 5KA mutation abrogate activation and polyubiquitination of RIG-I by reducing RNA biding activity of RIG-I. However, this possibility is weakened by following observations. First, the 5KA mutation caused near-complete loss of RIG-I activation, but the RIG-I-5KA mutant protein still possessed RNA binding activity. Second, overexpression of Riplet led to RIG-I activation in the absence of dsRNA in HEK293 cells, and this ligand-independent activation of RIG-I

(B) Expression vector for the two RIG-I N-terminal CARDs were transfected into wild-type or *Riplet*$^{-/-}$ MEFs together with reporter plasmids, and IFN-β promoter activation was examined by the reporter gene assay. Data are shown as means ±SD and are representative of three independent experiments. "NS" indicates not statistically significant.

(C) Empty, wild-type RIG-I-, or RIG-I-5KA mutant-expressing vectors were transfected into the *Riplet*$^{-/-}$ MEF cell line together with or without the Riplet-expressing vector. Cells were stimulated with HCV 3′UTR short dsRNA, and reporter gene assay was performed as described in (A).

(D) Empty or wild-type RIG-I-expressing vectors were transfected into the *Riplet*$^{-/-}$ MEF cell line together with empty, wild-type Riplet, or Riplet mutant (Riplet dRING)-expressing vector. Cells were stimulated with HCV 3′UTR short dsRNA, and the reporter gene assay was performed as described in (A).

(E) Empty or MDA5-expressing vectors was transfected into wild-type or *Riplet*$^{-/-}$ MEFs together with reporter plasmids, and after 24 hr IFN-β promoter activation was examined by the reporter gene assay.

(F–H) Of poly(I:C), 0.8 μg was transfected into wild-type or *Riplet*$^{-/-}$ MEFs. Twenty-four hours after transfection, total RNA was extracted from MEFs and subjected to RT-qPCR to determine IFN-β (F), Ccl5 (G), and IP10 (H) expression. Expression in each sample was normalized to the β-actin mRNA expression.

(I–K) Wild-type or *Riplet*$^{-/-}$ MEFs were stimulated with 1 μg of LPS. Total RNA was extracted at the indicated times and subjected to RT-qPCR analysis for of IFN-β (I), IL-6 (J), or IP-10 (K) expression.

(L) Wild-type or *Riplet*$^{-/-}$ MEFs were stimulated with LPS, and after 24 hr the amount of IL-6 in culture supernatants was measured by ELISA.

(M) HEK293FT cells were transfected with Riplet, FLAG-tagged RIG-I-CTD, and HA-tagged ubiquitin (HA-Ub) expression vectors. Twenty-four hours after transfection, cell lysates were extracted and immunoprecipitation was carried out with anti-FLAG antibody as previously described (Oshiumi et al., 2009). The samples were analyzed by SDS-PAGE, and western blotting was performed using anti-HA polyclonal antibody (Ub) and anit-Flag M2 monoclonal antibody (RIG-I-CTD). The plasmids are described previously (Oshiumi et al., 2009).

(N) Expression vector of dominant negative form of Riplet (Riplet DN) was transfected into HEK293FT cells together with expression vector of FLAG-tagged RIG-I CTD and HA-tagged ubiquitin. Cells were stimulated with dsRNA. Ubiquitination of RIG-I CTD was detected as in (M).

(O) R3T cells were transfected with Riplet, FLAG-tagged RIG-I-CTD, and HA-tagged ubiquitin (HA-Ub) expression vectors. Cells were stimulated with dsRNA. Ubiquitination of RIG-I-CTD was detected as in (M).

See also Figure S3.

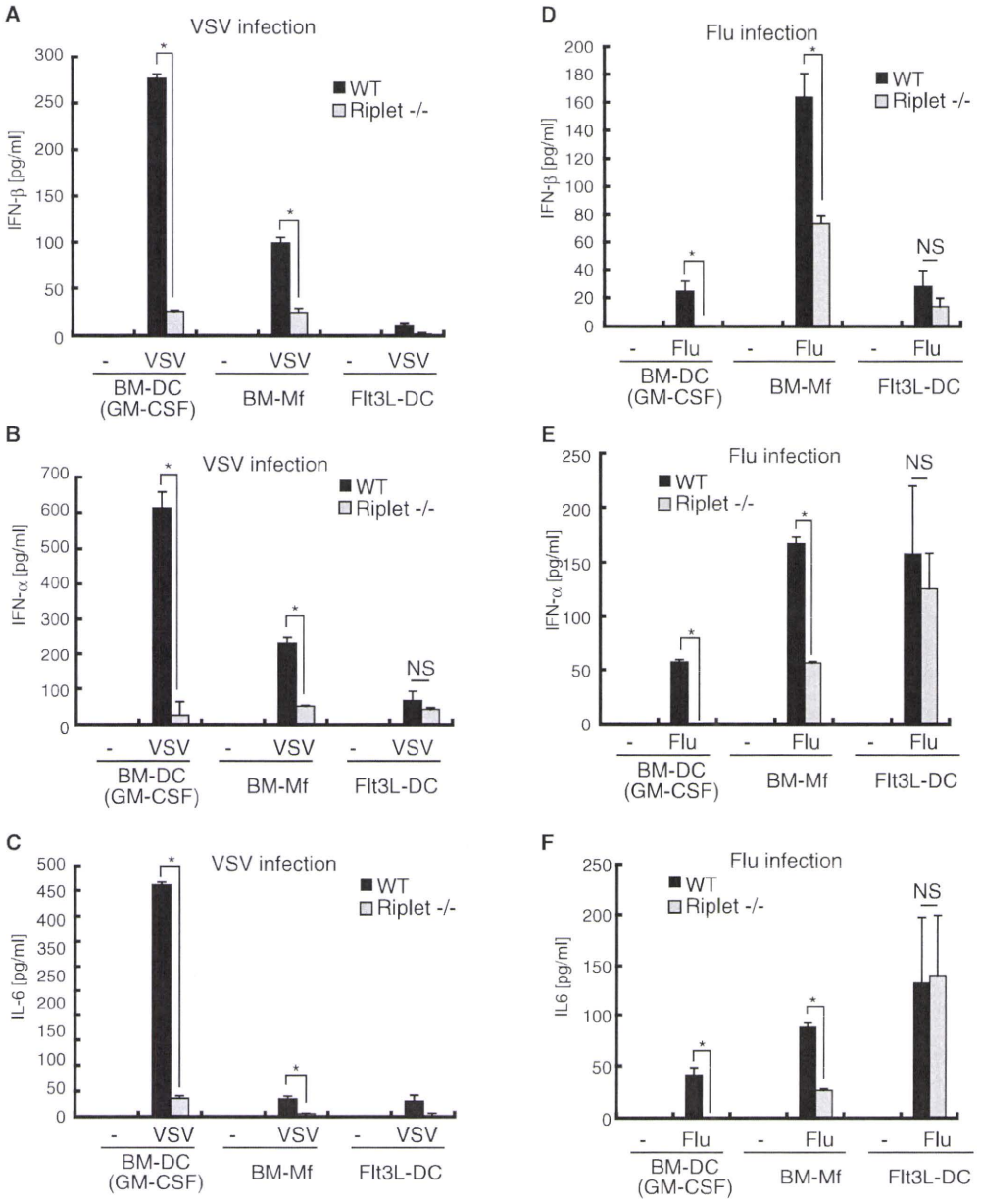

Figure 6. Role of Riplet in Responses to VSV or Flu Infection in Bone Marrow-Derived Cells

GM-DCs, BM-Mf, or Flt3L-DCs were induced from BM-derived cells in the presence of GM-CSF, M-CSF, or Flt3L and infected with VSV or influenza A virus at moi = 1. Twenty-four hours after viral infection, amounts of IFN-β (A and D), -α (B and E), and IL-6 (C and F) in culture supernatants were measured by ELISA. Data are shown as means ±SD and are representative of two independent experiments. *$p < 0.05$ (Student's t test). NS indicates not statistically significant.
See also Figure S4.

by overexpression of Riplet was also abolished by the 5KA mutation. These data support our model. However, we do not exclude the possibility that other Lys residues of RIG-I are ubiquitinated by Riplet, because we have not yet directly detected polyubiquitinated residues of RIG-I CTD by mass spectrometory analysis. Further in vitro studies are required to determine the polyubiquitination sites and to reveal precise RIG-I regulatory mechanisms by Riplet-mediated Lys63-linked polyubiquitation.

In general, E3 ubiquitin ligase targets several types of proteins. Therefore, it is possible that Riplet targets other proteins. Previous work has shown that Riplet binds to the Trk-fused gene (TFG) protein (Suzuki et al., 2001). The TFG protein interacts with TANK and NEMO, which are involved in the NF-κB pathway (Miranda et al., 2006). Although NEMO is involved in IPS-1-mediated signaling, RIG-I CARDs- or MDA5-mediated signaling was normal in *Riplet*$^{-/-}$ MEFs. Therefore, interaction between Riplet

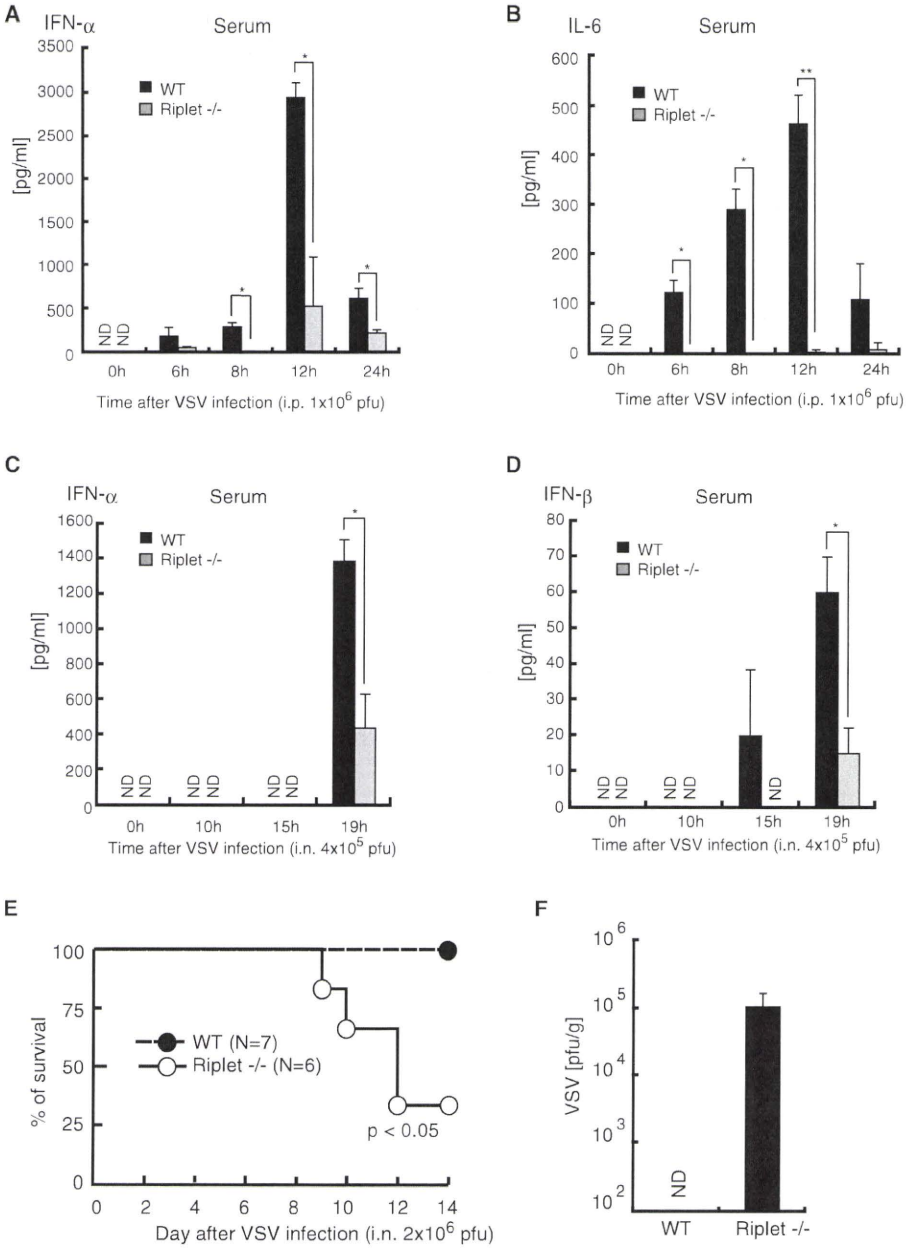

Figure 7. Role of Riplet in Antiviral Responses In Vivo

(A and B) Wild-type or *Riplet*$^{-/-}$ mice were injected intraperitoneally with 1 × 10^6 pfu of VSV. Amounts of IFN-α (A) and IL-6 (B) in mouse serum were measured by ELISA. Data are shown as mean ±SD of samples obtained from three wild-type and three Riplet −/− mice at each time point. *$p < 0.05$ (Student's t test). "ND" indicates not detected.

(C and D) Wild-type and *Riplet*$^{-/-}$ mice were infected intranasally with 4 × 10^5 pfu of VSV. Amounts of IFN-α (C) and IFN-β (D) in mouse serum were measured by ELISA.

(E) Wild-type and *Riplet*$^{-/-}$ mice were infected intranasally with 2 × 10^6 pfu of VSV and mice mortality was observed for 14 days (*$p < 0.05$ between wild-type and *Riplet*$^{-/-}$ mice, log rank test).

(F) Wild-type and *Riplet*$^{-/-}$ mice were infected intranasally with 2 × 10^6 pfu of VSV, and sacrificed for their tissues on day 7 after infection. Titers in brain were determined by the plaque assay. Viral titers in brains of wild-type mice were below 100 pfu/g, and thus not detected (ND). Data are shown as means ±SD (n = 3). See also Figure S5.

and TFG protein is not required for RIG-I-mediated signaling. However, since TFG is involved in tumorigenesis (Miranda et al., 2006), Riplet may be involved in human tumorigenesis.

Several viral proteins inhibit RIG-I-mediated signaling. For example, Flu NS1 inhibits TRIM25 and HCV NS3/4A cleaves IPS-1 (Meylan et al., 2005; Gack et al., 2009). Therefore, Riplet may be inhibited by viral proteins. Indeed, our pilot study indicated that the Riplet protein is disrupted in human hepatocyte cell lines carrying a full-length HCV replicon. RIG-I is involved in innate immune responses against various viruses. In this study, we showed that Riplet is required for innate immune responses against VSV, Flu, and SeV. Therefore, Riplet is also expected to be involved in innate immune responses against other viruses that are recognized by RIG-I.

EXPERIMENTAL PROCEDURES

Generation of Riplet-Deficient Mice

The Riplet gene was amplified by PCR using genomic DNA extracted from ESCs by PCR. The targeting vector was constructed by replacing the second and third exons with a neomycine-resistance gene cassette (Neo), and a herpes simplex virus thymidine kinase (HSV-TK) driven by PGK promoter was inserted into the genomic fragment for negative selection. After the targeting vector was transfected into 129/Sv mice-derived ESCs, G418 and gancyclovir doubly resistant colonies were selected and screened by PCR. The targeted cell line was injected in C57BL/6 blastocysts, resulting in the birth of male chimeric mice. These mice were then crossed with 129/Sv mice to obtain heterozygous mutants. The heterozygous mutants were intercrossed to obtain homozygous *Riplet*$^{-/-}$ mice.

Cells, Viruses, and Reagents

Wild-type and *Riplet*$^{-/-}$ MEFs were prepared from day 12.5–13.5 embryos. *Riplet*$^{-/-}$ MEFs were immortalized with large T antigen and named R3T cell line. BM cells were prepared from 5- to 10-week-old mice. VSV Indiana strain was provided by A. Takada (Hokkaido University). VSV was amplified using Vero cells and the viral titer was determined by the plaque assay. Flu (PR8 strain) and SeV (HVJ strain) was provided by Y. Sakoda (Hokkaido University). HSV-1 strain was provided by K. Kondo (The JIKEI University). Anti-mouse IRF3 antibody was purchased from Zymed. Anti-phospho-STAT1 antibody was purchased from Cell Signaling and anti-STAT1 antibody from Santa Cruz. Salomon sperm dsDNA was purchased from Invitrogen. To determine the viral titer in the brain, the mice were sacrificed, and the brain was aseptically removed and frozen at −80°C. The brain was homogenized in 1 ml of PBS on ice, and the titer was determined by plaque assay.

Preparation of Viral Double-Stranded RNA

cDNA of the HCV 3′UTR region was amplified from total RNA of the HCV genotype 1b full-length replicon using primers HCV-F1 and HCV-R1, and then cloned in the pGEM-T Easy Vector. The primer set sequences were HCV-F1, CTCCAGGTGAGATCAATAGG; and HCV-R1, CGTGACTAGGGCTAAGATGG. RNA was synthesized using T7 and SP6 RNA polymerases. Template DNA was digested by DNase I, and RNA was purified using TRIZOL (Invitrogen) according to manufacturer's instructions.

Quantitative PCR

For qPCR, total RNA was extracted with TRIZOL (Invitrogen) and 0.5 μg of RNA was reverse-transcribed using the High Capacity cDNA Transcription Kit (ABI) with random primers according to the manufacturer's instructions. qPCR was performed using the Step One Real-Time PCR system (ABI). Primer sequences used for qPCR are listed in Table S1.

Measurement of Cytokines

In brief, 5 × 10^5 cells in a 24-well plate were either infected with VSV or Flu, stimulated with LPS, or transfected with HCV 3′UTR dsRNA or poly(I:C). Twenty-four hours after infection, stimulation, or transfection, culture supernatants were collected and analyzed for IFN-α, -β, and IL-6 production by ELISA. Cytokine levels were measured in mouse serum obtained from the mouse tail vein. ELISA kits for mouse IFN-α and -β were purchased from PBL Biomedical Laboratories. ELSA kit for mouse IL-6 was purchased from Invitrogen.

Preparation of Dendritic Cells and Macrophages

BM cells were prepared from the femur and tibia. The cells were cultured in RPMI1640 medium supplemented with 10% FCS, 100 μM 2-Me, and 100 ng/ml human Flt3 ligand (Pepro Tech), and 10 ng/ml murine GM-CSF or culture supernatant NIH 3T3 expressing M-CSF. After 6 days, cells were collected and used as Flt3L-DC, GM-DC, or BM-Mf. In the case of GM-DC or BM-Mf, the medium was changed every 2 days.

Native PAGE Analysis

Approximately 1 × 10^6 MEFs were infected with VSV at moi = 1 for 9 hr and then lysed. Cell lysates in native PAGE sample buffer (62.5 mM Tris-HCl [pH 6.8], 15% glycerol, and BPB) were separated using native PAGE and then immunoblotted with anti-murine IRF3 antibody (Zymed).

Luciferase Assay

Expression plasmids for mouse RIG-I N-terminal CARDs, full-length RIG-I, or full-length MDA5 were constructed in pEF-BOS. The cDNA fragment encoding the ORF of RIG-I or MDA5 was amplified by RT-PCR using total RNA prepared from MEFs. The Riplet dRING mutant protein lacks 1–69 aa region. Wild-type and mutant (Riplet dRING) Riplet-expression vectors were described previously (Oshiumi et al., 2009). Wild-type or *Riplet*$^{-/-}$ MEFs were transiently transfected in 24-well plates with reporter constructs containing the IFN-β promoter and Renilla luciferase (internal control) together with the empty vector (control), RIG-I CARDs, full-length RIG-I, or MDA5 expression vectors. Twenty-four hours after transfection, cells were lysed and subjected to the luciferase assay using the Dual-Luciferase Reporter Assay system (Promega).

Statistical Analyses

Statistical significance of differences between groups was determined by the Student's t test, and survival curves were analyzed by the log rank test using Prism 4 for Macintosh software (GraphPad Sofware, Inc.). Chi-square goodness-of-fit tests and Student's t tests were performed using MS-Excel software and a chi-square distribution table.

SUPPLEMENTAL INFORMATION

Supplemental Information includes five figures, one table, and Supplemental Experimental Procedures and can be found with this article at doi:10.1016/j.chom.2010.11.008.

ACKNOWLEDGMENTS

We thank Dr. John P. Atkinson (Washington University) and Dr. Ralph Steinman (Rockefeller University) for critical discussions, Yoko Esaki and Kiyo Kawata for technical support in generating Riplet KO mice, N. Irie for a pilot study of B-DNA stimulation assay, and Sakoda Y. for technical instructions for the experiments using Flu and SeV. This work was supported in part by the Mitsubishi Foundation; Mochida Foundation; Akiyama Life Science Foundation; and Grants-in-Aid from Ministry of Education, Science, and Culture and Ministry of Health, Labor, and Welfare of Japan.

Received: June 4, 2010
Revised: August 18, 2010
Accepted: November 5, 2010
Published: December 15, 2010

REFERENCES

Akira, S., Uematsu, S., and Takeuchi, O. (2006). Pathogen recognition and innate immunity. Cell *124*, 783–801.

Arimoto, K., Takahashi, H., Hishiki, T., Konishi, H., Fujita, T., and Shimotohno, K. (2007). Negative regulation of the RIG-I signaling by the ubiquitin ligase RNF125. Proc. Natl. Acad. Sci. USA *104*, 7500–7505.

Chiu, Y.H., Macmillan, J.B., and Chen, Z.J. (2009). RNA polymerase III detects cytosolic DNA and induces type I interferons through the RIG-I pathway. Cell *138*, 576–591.

Cui, S., Eisenacher, K., Kirchhofer, A., Brzozka, K., Lammens, A., Lammens, K., Fujita, T., Conzelmann, K.K., Krug, A., and Hopfner, K.P. (2008). The C-terminal regulatory domain is the RNA 5′-triphosphate sensor of RIG-I. Mol. Cell *29*, 169–179.

Diebold, S.S., Kaisho, T., Hemmi, H., Akira, S., and Reis e Sousa, C. (2004). Innate antiviral responses by means of TLR7-mediated recognition of single-stranded RNA. Science *303*, 1529–1531.

Douglas, J., Cilliers, D., Coleman, K., Tatton-Brown, K., Barker, K., Bernhard, B., Burn, J., Huson, S., Josifova, D., Lacombe, D., et al. (2007). Mutations in RNF135, a gene within the NF1 microdeletion region, cause phenotypic abnormalities including overgrowth. Nat. Genet. *39*, 963–965.

Gack, M.U., Shin, Y.C., Joo, C.H., Urano, T., Liang, C., Sun, L., Takeuchi, O., Akira, S., Chen, Z., Inoue, S., and Jung, J.U. (2007). TRIM25 RING-finger E3 ubiquitin ligase is essential for RIG-I-mediated antiviral activity. Nature *446*, 916–920.

Gack, M.U., Kirchhofer, A., Shin, Y.C., Inn, K.S., Liang, C., Cui, S., Myong, S., Ha, T., Hopfner, K.P., and Jung, J.U. (2008). Roles of RIG-I N-terminal tandem CARD and splice variant in TRIM25-mediated antiviral signal transduction. Proc. Natl. Acad. Sci. USA *105*, 16743–16748.

Gack, M.U., Albrecht, R.A., Urano, T., Inn, K.S., Huang, I.C., Carnero, E., Farzan, M., Inoue, S., Jung, J.U., and Garcia-Sastre, A. (2009). Influenza A virus NS1 targets the ubiquitin ligase TRIM25 to evade recognition by the host viral RNA sensor RIG-I. Cell Host Microbe *5*, 439–449.

Gao, D., Yang, Y.K., Wang, R.P., Zhou, X., Diao, F.C., Li, M.D., Zhai, Z.H., Jiang, Z.F., and Chen, D.Y. (2009). REUL is a novel E3 ubiquitin ligase and stimulator of retinoic-acid-inducible gene-I. PLoS ONE *4*, e5760. 10.1371/journal.pone.0005760.

Honda, K., Yanai, H., Takaoka, A., and Taniguchi, T. (2005). Regulation of the type I IFN induction: a current view. Int. Immunol. *17*, 1367–1378.

Honda, K., Takaoka, A., and Taniguchi, T. (2006). Type I interferon [corrected] gene induction by the interferon regulatory factor family of transcription factors. Immunity *25*, 349–360.

Horner, S.M., and Gale, M., Jr. (2009). Intracellular innate immune cascades and interferon defenses that control hepatitis C virus. J. Interferon Cytokine Res. *29*, 489–498.

Hornung, V., Ellegast, J., Kim, S., Brzozka, K., Jung, A., Kato, H., Poeck, H., Akira, S., Conzelmann, K.K., Schlee, M., et al. (2006). 5′-Triphosphate RNA is the ligand for RIG-I. Science *314*, 994–997.

Ishii, K.J., Coban, C., Kato, H., Takahashi, K., Torii, Y., Takeshita, F., Ludwig, H., Sutter, G., Suzuki, K., Hemmi, H., et al. (2006). A Toll-like receptor-independent antiviral response induced by double-stranded B-form DNA. Nat. Immunol. *7*, 40–48.

Ishii, K.J., Kawagoe, T., Koyama, S., Matsui, K., Kumar, H., Kawai, T., Uematsu, S., Takeuchi, O., Takeshita, F., Coban, C., and Akira, S. (2008). TANK-binding kinase-1 delineates innate and adaptive immune responses to DNA vaccines. Nature *451*, 725–729.

Ishikawa, H., and Barber, G.N. (2008). STING is an endoplasmic reticulum adaptor that facilitates innate immune signalling. Nature *455*, 674–678.

Ishikawa, H., Ma, Z., and Barber, G.N. (2009). STING regulates intracellular DNA-mediated, type I interferon-dependent innate immunity. Nature *461*, 788–792.

Kato, H., Sato, S., Yoneyama, M., Yamamoto, M., Uematsu, S., Matsui, K., Tsujimura, T., Takeda, K., Fujita, T., Takeuchi, O., and Akira, S. (2005). Cell type-specific involvement of RIG-I in antiviral response. Immunity *23*, 19–28.

Kato, H., Takeuchi, O., Sato, S., Yoneyama, M., Yamamoto, M., Matsui, K., Uematsu, S., Jung, A., Kawai, T., Ishii, K.J., et al. (2006). Differential roles of MDA5 and RIG-I helicases in the recognition of RNA viruses. Nature *441*, 101–105.

Kawai, T., Takahashi, K., Sato, S., Coban, C., Kumar, H., Kato, H., Ishii, K.J., Takeuchi, O., and Akira, S. (2005). IPS-1, an adaptor triggering RIG-I- and Mda5-mediated type I interferon induction. Nat. Immunol. *6*, 981–988.

Kumagai, Y., Takeuchi, O., Kato, H., Kumar, H., Matsui, K., Morii, E., Aozasa, K., Kawai, T., and Akira, S. (2007). Alveolar macrophages are the primary interferon-alpha producer in pulmonary infection with RNA viruses. Immunity *27*, 240–252.

Kumar, H., Kawai, T., Kato, H., Sato, S., Takahashi, K., Coban, C., Yamamoto, M., Uematsu, S., Ishii, K.J., Takeuchi, O., and Akira, S. (2006). Essential role of IPS-1 in innate immune responses against RNA viruses. J. Exp. Med. *203*, 1795–1803.

Meylan, E., Curran, J., Hofmann, K., Moradpour, D., Binder, M., Bartenschlager, R., and Tschopp, J. (2005). Cardif is an adaptor protein in the RIG-I antiviral pathway and is targeted by hepatitis C virus. Nature *437*, 1167–1172.

Miranda, C., Roccato, E., Raho, G., Pagliardini, S., Pierotti, M.A., and Greco, A. (2006). The TFG protein, involved in oncogenic rearrangements, interacts with TANK and NEMO, two proteins involved in the NF-kappaB pathway. J. Cell. Physiol. *208*, 154–160.

Nakhaei, P., Genin, P., Civas, A., and Hiscott, J. (2009). RIG-I-like receptors: sensing and responding to RNA virus infection. Semin. Immunol. *21*, 215–222.

Onoguchi, K., Yoneyama, M., Takemura, A., Akira, S., Taniguchi, T., Namiki, H., and Fujita, T. (2007). Viral infections activate types I and III interferon genes through a common mechanism. J. Biol. Chem. *282*, 7576–7581.

Oshiumi, H., Matsumoto, M., Hatakeyama, S., and Seya, T. (2009). Riplet/RNF135, a RING finger protein, ubiquitinates RIG-I to promote interferon-beta induction during the early phase of viral infection. J. Biol. Chem. *284*, 807–817.

Pichlmair, A., Schulz, O., Tan, C.P., Naslund, T.I., Liljestrom, P., Weber, F., and Reis e Sousa, C. (2006). RIG-I-mediated antiviral responses to single-stranded RNA bearing 5′-phosphates. Science *314*, 997–1001.

Rehwinkel, J., Tan, C.P., Goubau, D., Schulz, O., Pichlmair, A., Bier, K., Robb, N., Vreede, F., Barclay, W., Fodor, E., and Reis e Sousa, C. (2010). RIG-I detects viral genomic RNA during negative-strand RNA virus infection. Cell *140*, 397–408.

Saito, T., Hirai, R., Loo, Y.M., Owen, D., Johnson, C.L., Sinha, S.C., Akira, S., Fujita, T., and Gale, M., Jr. (2007). Regulation of innate antiviral defenses through a shared repressor domain in RIG-I and LGP2. Proc. Natl. Acad. Sci. USA *104*, 582–587.

Saito, T., Owen, D.M., Jiang, F., Marcotrigiano, J., and Gale, M., Jr. (2008). Innate immunity induced by composition-dependent RIG-I recognition of hepatitis C virus RNA. Nature *454*, 523–527.

Seth, R.B., Sun, L., Ea, C.K., and Chen, Z.J. (2005). Identification and characterization of MAVS, a mitochondrial antiviral signaling protein that activates NF-kappaB and IRF 3. Cell *122*, 669–682.

Shigemoto, T., Kageyama, M., Hirai, R., Zheng, J., Yoneyama, M., and Fujita, T. (2009). Identification of loss of function mutations in human genes encoding RIG-I and MDA5: implications for resistance to type I diabetes. J. Biol. Chem. *284*, 13348–13354.

Sun, Q., Sun, L., Liu, H.H., Chen, X., Seth, R.B., Forman, J., and Chen, Z.J. (2006). The specific and essential role of MAVS in antiviral innate immune responses. Immunity *24*, 633–642.

Suzuki, H., Fukunishi, Y., Kagawa, I., Saito, R., Oda, H., Endo, T., Kondo, S., Bono, H., Okazaki, Y., and Hayashizaki, Y. (2001). Protein-protein interaction panel using mouse full-length cDNAs. Genome Res. *11*, 1758–1765.

Takahasi, K., Yoneyama, M., Nishihori, T., Hirai, R., Kumeta, H., Narita, R., Gale, M., Jr., Inagaki, F., and Fujita, T. (2008). Nonself RNA-sensing mechanism of RIG-I helicase and activation of antiviral immune responses. Mol. Cell *29*, 428–440.

Takeuchi, O., and Akira, S. (2010). Pattern recognition receptors and inflammation. Cell *140*, 805–820.

Xu, L.G., Wang, Y.Y., Han, K.J., Li, L.Y., Zhai, Z., and Shu, H.B. (2005). VISA is an adapter protein required for virus-triggered IFN-beta signaling. Mol. Cell *19*, 727–740.

Yoneyama, M., and Fujita, T. (2009). RNA recognition and signal transduction by RIG-I-like receptors. Immunol. Rev. *227*, 54–65.

Yoneyama, M., and Fujita, T. (2010). Recognition of viral nucleic acids in innate immunity. Rev. Med. Virol. *20*, 4–22.

Yoneyama, M., Kikuchi, M., Natsukawa, T., Shinobu, N., Imaizumi, T., Miyagishi, M., Taira, K., Akira, S., and Fujita, T. (2004). The RNA helicase RIG-I has an essential function in double-stranded RNA-induced innate antiviral responses. Nat. Immunol. *5*, 730–737.

Zeng, W., Sun, L., Jiang, X., Chen, X., Hou, F., Adhikari, A., Xu, M., and Chen, Z.J. (2010). Reconstitution of the RIG-I pathway reveals a signaling role of unanchored polyubiquitin chains in innate immunity. Cell *141*, 315–330.

Hepatitis C Virus Core Protein Abrogates the DDX3 Function That Enhances IPS-1-Mediated IFN–Beta Induction

Hiroyuki Oshiumi[1], Masanori Ikeda[2], Misako Matsumoto[1], Ayako Watanabe[1], Osamu Takeuchi[3], Shizuo Akira[3], Nobuyuki Kato[2], Kunitada Shimotohno[4], Tsukasa Seya[1]*

1 Department of Microbiology and Immunology, Hokkaido University Graduate School of Medicine, Sapporo, Japan, **2** Department of Tumor Virology, Okayama University Graduate School of Medicine, Dentistry, and Pharmaceutical Sciences, Okayama, Japan, **3** Laboratory of Host Defense, WPI Immunology Frontier Research Center, Research Institute for Microbial Diseases, Osaka University, Suita, Japan, **4** Research Institute, Chiba Institute of Technology, Narashino, Japan

Abstract

The DEAD box helicase DDX3 assembles IPS-1 (also called Cardif, MAVS, or VISA) in non-infected human cells where minimal amounts of the RIG-I-like receptor (RLR) protein are expressed. DDX3 C-terminal regions directly bind the IPS-1 CARD-like domain as well as the N-terminal hepatitis C virus (HCV) core protein. DDX3 physically binds viral RNA to form IPS-1-containing spots, that are visible by confocal microscopy. HCV polyU/UC induced IPS-1-mediated interferon (IFN)-beta promoter activation, which was augmented by co-transfected DDX3. DDX3 spots localized near the lipid droplets (LDs) where HCV particles were generated. Here, we report that HCV core protein interferes with DDX3-enhanced IPS-1 signaling in HEK293 cells and in hepatocyte Oc cells. Unlike the DEAD box helicases RIG-I and MDA5, DDX3 was constitutively expressed and colocalized with IPS-1 around mitochondria. In hepatocytes (O cells) with the HCV replicon, however, DDX3/IPS-1-enhanced IFN-beta-induction was largely abrogated even when DDX3 was co-expressed. DDX3 spots barely merged with IPS-1, and partly assembled in the HCV core protein located near the LD in O cells, though in some O cells IPS-1 was diminished or disseminated apart from mitochondria. Expression of DDX3 in replicon-negative or core-less replicon-positive cells failed to cause complex formation or LD association. HCV core protein and DDX3 partially colocalized only in replicon-expressing cells. Since the HCV core protein has been reported to promote HCV replication through binding to DDX3, the core protein appears to switch DDX3 from an IFN-inducing mode to an HCV-replication mode. The results enable us to conclude that HCV infection is promoted by modulating the dual function of DDX3.

Citation: Oshiumi H, Ikeda M, Matsumoto M, Watanabe A, Takeuchi O, et al. (2010) Hepatitis C Virus Core Protein Abrogates the DDX3 Function That Enhances IPS-1-Mediated IFN–Beta Induction. PLoS ONE 5(12): e14258. doi:10.1371/journal.pone.0014258

Editor: Jörn Coers, Duke University Medical Center, United States of America

Received May 28, 2010; **Accepted** November 16, 2010; **Published** December 8, 2010

Funding: This work was supported in part by the Program of Founding Research Centers for Emerging and Reemerging Infectious Diseases, MEXT, Sapporo Biocluster "Bio-S", the Knowledge Cluster Initiative of the MEXT, Grants-in-Aid from the Ministry of Education, Science, and Culture (Specified Project for Advanced Research) and the Ministry of Health, Labor, and Welfare of Japan, Mochida Foundation, Yakult Foundation, NorthTec Foundation and Waxman Foundation. The funders had no role in study design, data collection and analysis, decision to publish, or preparation of the manuscript.

Competing Interests: The authors have declared that no competing interests exist.

* E-mail: seya-tu@pop.med.hokudai.ac.jp

Introduction

The retinoic acid inducible gene-I (RIG-I) and the melanoma differentiation-associated gene 5 (MDA5) encode cytoplasmic RNA helicases [1–3] that signal the presence of viral RNA through the adaptor, IPS-1/Mitochondrial antiviral signaling protein (MAVS)/Caspase recruitment domain (CARD) adaptor inducing interferon (IFN)-beta (Cardif)/Virus-induced signaling adaptor (VISA) to produce IFN-beta [4–7]. IPS-1 is localized to the mitochondrial outer membrane through its C-terminus [6]. Increasing evidence suggests that the DEAD-box RNA helicase DDX3, which is on the X chromosome, participates in the regulation of type I IFN induction by the RIG-I pathway.

DDX3 acts on the IFN-inducing pathway by a complex mechanism. Early studies reported that DDX3 up-regulates IFN-beta induction by interacting with IKKepsilon [8] or TBK1 [9] in a kinase complex. Both TBK1 and IKKepsilon are IRF-3-activating kinases with NF-kappaB- and IFN-inducible properties. DDX3 has been proposed to bind IKKepsilon, and IKKepsilon is generated after NF-kappaB activation [10]. Yeast two-hybrid studies demonstrated that DDX3 binds IPS-1, and both are constitutively present prior to infection (Fig. 1). Ultimately, DDX3 forms a complex with the DEAD-box RNA helicases RIG-I and MDA5 [11], which are present at only low amounts in resting cells, and are up-regulated during virus infection. Previously we used gene silencing and disruption, to show that the main function of DDX3 is to interact with viral RNA and enhance RIG-I signaling upstream of NAP1/TBK1/IKKepsilon [11]. Hence, DDX3 is involved in multiple pathways of RNA sensing and signaling during viral infection.

DDX3 resides in both the nucleus and the cytoplasm [12], and has been implicated in a variety of processes in gene expression regulation, including transcription, splicing, mRNA export, and translation [13]. A recent report suggested that the N-terminus of hepatitis C virus (HCV) core protein binds the C-terminus of DDX3 (Fig. S1) [14,15], and this interaction is required for HCV replication [16]. Although DDX3 promotes efficient HCV infection by accelerating HCV RNA replication, the processes

A

Two representative polyI:C-binding proteins identified by mass-spectrometric analysis

dsRNA-binding protein	ID	Mr (kDa)	polyI:C	polyU	gene name
dsRNA-activated protein kinase	IPI00019463	63 kDa	37	2	PKR
ATP-dependent RNA helicase	IPI00215637	73 kDa	19	12	DDX3

B

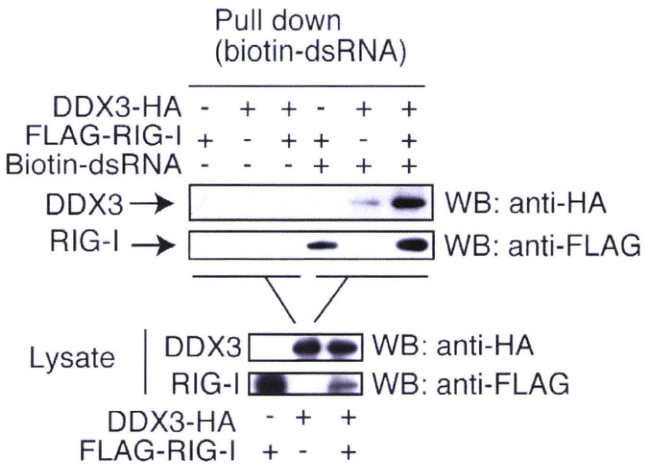

Figure 1. DDX3 is a RNA-binding protein. (A) DDX3 is a polyU- and polyI:C-binding protein. Mass spectrometry analyses indicated that DDX3 binds polyI:C- and polyU-Sepharose, although PKR binds polyI:C but not polyU. The rough data from MASCOT and one representative of six trials are shown. (B) DDX3 binds dsRNA, RIG-I and HCV core protein. Expression vectors for Flag-tagged RIG-I and HA-tagged DDX3 were transfected into HEK293 cells using lipofectamine 2000. Twenty-four hours after the transfection, extract from transfected cells were mixed with biotin-conjugated dsRNA. RNA-protein complex were recovered by pull-down assay using streptavidin-Sepharose. The protein within the pull-down fraction was analyzed by western blotting. The results are representative of two independent experiments.
doi:10.1371/journal.pone.0014258.g001

appear independent of its interaction with the viral core protein [15]. HCV seems to co-opt DDX3, and require DDX3 for replication. In addition, the association between DDX3 and core protein implicates DDX3 in HCV-related hepatocellular carcinoma progression [17]. Therefore, DDX3 could be a novel target for the development of drugs against HCV [18].

A number of reports have demonstrated the formation of the DDX3-core protein complex in the cytoplasm, but the functional relevance of DDX3-core protein interaction is not known. In this report, we show evidence that the HCV core protein participates in suppression of DDX3-augmented IPS-1 signaling for IFN-β induction. Several possible functions of DDX3 are discussed, focusing on its core protein association and IPS-1-regulatory properties.

Materials and Methods

Cell culture and reagents

HEK293 cells and HEK293FT cells were maintained in Dulbecco's Modified Eagle's low or high glucose medium (Invitrogen, Carlsbad, CA) supplemented with 10% heat-inactivated FCS (Invitrogen) and antibiotics. Huh7.5 cells were maintained in MEM (Nissui, Tokyo, Japan) supplemented with 10% heat-inactivated FCS. Hepatocyte sublines with HCV replicon (O cells) and without replicon (Oc cells) were established as described previously [19]. O cells with core-less subgenomic replicon (sO cells) were also generated in Dr. Kato's laboratory [16,19]. RIG-I −/− mouse embryonic fibroblasts (MEF) were gifts from Drs. Takeuchi and Akira [1]. Anti-FLAG M2 monoclonal Ab and anti-HA polyclonal Ab were purchased from Sigma. A mitochondria marker (Mitotracker) and Alexa Fluor®-conjugated secondary antibodies were purchased from Molecular probe. Anti-HCV core mAb (C7-50) [20] and anti-human DDX3 pAb were from Affinity BioReagents, Inc and Abcam, Cambridge MA, respectively.

Plasmids

DDX3 cDNA encoding the entire ORF was cloned into pCR-blunt vector using primers, DDX3N F-Xh (CTC GAG CCA CCA TGA GTC ATG TGG CAG TGG AA) and DDX3C R-Ba (GGA TCC GTT ACC CCA CCA GTC AAC CCC) from human lung cDNA library. To make an expression plasmid, HA tag was fused at the C-terminal end of the full length DDX3 (pEF-BOS DDX3-HA). pEF-BOS DDX3 (1-224aa) vector was made by using primers,

DDX3 N-F-Xh and DDX3D1 (GGA TCC GGC ACA AGC CAT CAA GTC TCT TTT C). pEF-BOS DDX3-HA (225-662) was made by using primers, DDX3D2-3 (CTC GAG CCA CCA TGC AAA CAG GGT CTG GAA AAA C) and DDX3C R-Ba. To make pEF-BOS DDX3-HA (225-484) and pEF-BOS DDX3-HA (485-663), the primers, DDX3D2 R-Ba (GGA TCC AAG GGC CTC TTC TCT ATC CCT C) and DDX3D3 F-Xh (CTC GAG CCA CCA TGC ACC AGT TCC GCT CAG GAA AAA G) were used, respectively. HCV core expressing plasmids, pcDNA3.1 HCVO core or JFH1 core, were previously reported by N. Kato (Okayama University Japan) [16]. Another 1b genotype of the core was cloned from a HCV patient in Osaka Medical Center (Osaka) according to the recommendation of the Ethical Committee in Osaka. We obtained written informed consent from each patient for research use of their samples. Reporter and internal control plasmids for reporter gene assay are previously described [21,22].

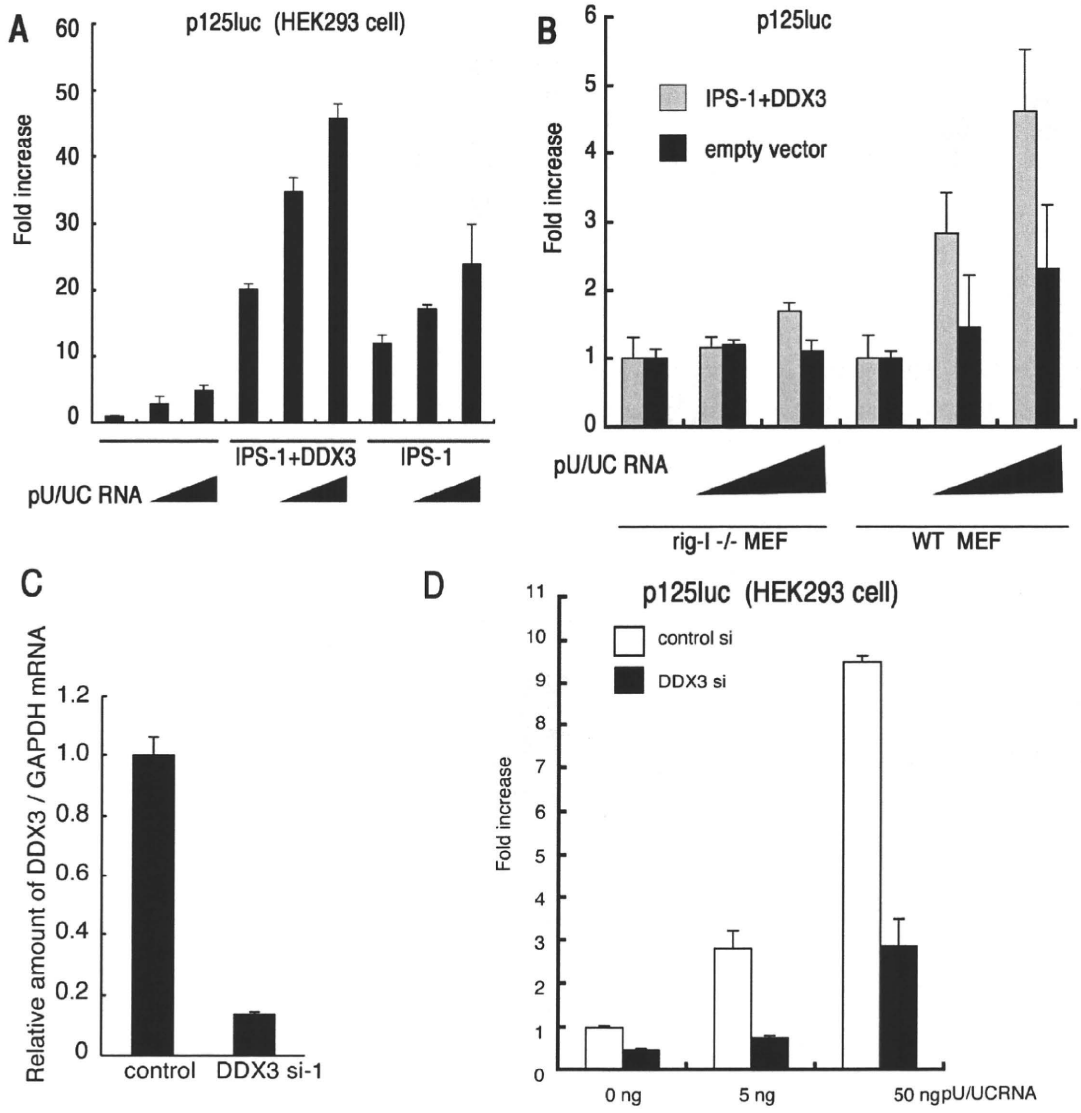

Figure 2. DDX3 is a positive regulator of IPS-1-mediated IFN promoter activation. (A) IFN-β induction by polyU/UC is augmented by DDX3. IPS-1 (100 ng), DDX3 (100 ng) and p125luc reporter (100 ng) plasmids were transfected into HEK293 cells in 24-well plates with or without the HCV 3′ UTR poly U/UC region (PU/UC) RNA (0, 25 or 50 ng/well), synthesized *in vitro* by T7 RNA polymerase. HCV RNA-enhancing activation of IFN-beta promoter was assessed by reporter assay in the presence or absence of the DDX3-IPS-1 complex. (B) RIG-I is essential for the DDX3/IPS-1-mediated IFN-promoter activation. MEF from wild-type and RIG-I −/− mice were transfected with plasmids of IPS-1, DDX3 and p125luc as in panel A, and stimulated with polyU/UC (0, 25 or 50 ng/well). Reporter activity was determined as in panel A. (C) Knockdown of DDX3. Negative control or DDX3 targeting siRNA (20 pmol), DDX3 si-1, was transfected into HEK293 cells, and after 48 hrs, expression of endogenous DDX3 mRNA was examined by real-time RT-PCR. DDX3 si-1-mediated down-regulation of the DDX3 protein was also confirmed by Western blotting (data not shown). (D) DDX3 enhances RIG-I-mediated IFN-beta promoter activation induced by polyU/UC. DDX3 si-1 or control siRNA was transfected into HEK293 cells with reporter plasmids (100 ng). After 48 hrs, cells were stimulated with polyU/UC (5~50 ng/ml) with lipofectamin 2000 reagent for 6 hrs, and activation of the reporter p125luc was measured. The results are representative of at least two independent experiments, each performed in triplicate.
doi:10.1371/journal.pone.0014258.g002

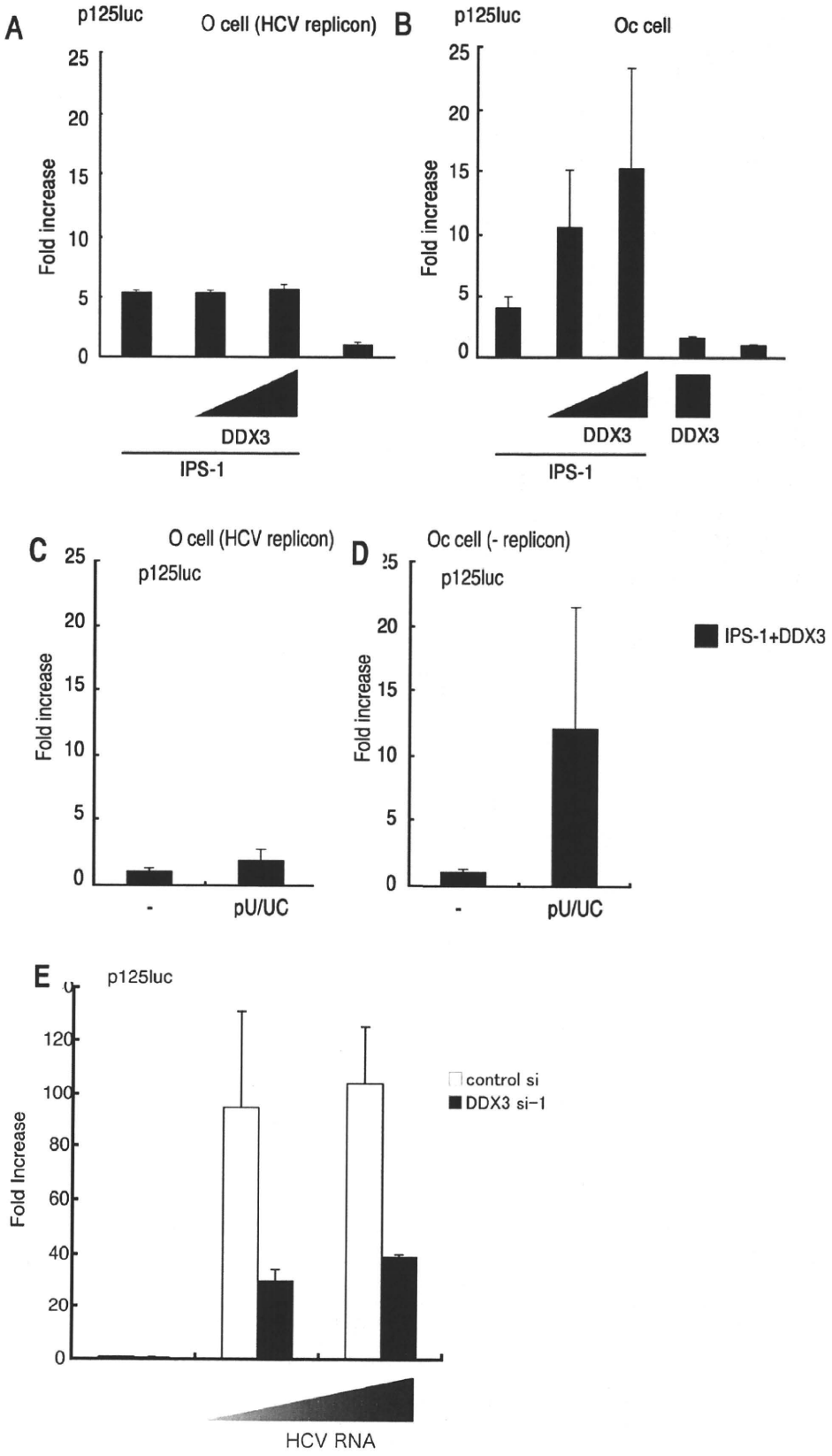
A
p125luc
O cell (HCV replicon)
Fold increase
25
20
15
10
5
0
DDX3
IPS-1
B
p125luc
Oc cell
Fold increase
25
20
15
10
5
0
DDX3
DDX3
IPS-1
C
O cell (HCV replicon)
p125luc
Fold increase
25
20
15
10
5
0
-
pU/UC
D
Oc cell (- replicon)
p125luc
Fold increase
25
20
15
10
5
0
-
pU/UC
IPS-1+DDX3
E
p125luc
Fold Increase
120
100
80
60
40
20
0
control si
DDX3 si-1
HCV RNA

Figure 3. The HCV replicon suppresses IPS-1/DDX3-mediated augmentation of IFN promoter activation. (A,B) O cells with the HCV replicon fail to activate an IFN-β reporter in response to IPS-1/DDX3. O cells contain the full-length HCV replicon, and Oc cells do not [16]. O cells (A) or Oc cells (B) were transfected with IPS-1, DDX3 or p125luc reporter plasmids. At timed intervals (24 hrs), reporter activity was determined as in Fig. 2. (C,D) The HCV replicon suppresses IFN-promoter activation by polyU/UC. O cells and Oc cells expressing IPS-1 and DDX3 were stimulated with polyU/UC. At 48 hrs, reporter activity was determined as in panel A. (E) DDX3 is required for enhanced activation of IFN-beta promoter by O cell HCV 3′UTR. HCV 3′ UTR cDNA was amplified by RT-PCR from RNA extracted from O cells containing full-length HCV replicon. The HCV 3′ UTR RNA was synthesized *in vitro* using T7 RNA polymerase. DDX3 siRNA or control siRNA was transfected into HEK293 cells with the p125luc reporter. After 24 hrs, cells were transfected with HCV RNA, and incubated for 24 hrs. The IFN-beta promoter activation was assessed by luciferase reporter assay. One representative of at least three independent experiments, each performed in triplicate, is shown.
doi:10.1371/journal.pone.0014258.g003

Preparation of HCV polyU/UC RNA

The HCV genotype 1b polyU/UC RNA (from 9421 to 9480, Accession number: EU867431) [23] was synthesized by T7 RNA polymerase *in vitro*. The template dsDNA sequences were; Forward: TAA TAC GAC TCA CTA TAG GGT TCC CTT TTT TTT TTT CTT TTT TTT TTT TTT TTT TTT TTT TTT CTC CTT TTT TTT TC, Reverse: GAA AAA AAA AGG AGA AAA AAA AAA AAA AAA AAA AAA AAA AGA AAA AAA AAA AGG GAA CCC TAT AGT GAG TCG TAT TA. The synthesized RNA was purified by TRIZOL reagent (Invitrogen). cDNA of HCV 3′ UTR region was amplified from total RNA of O cells using primers HCV-F1 and HCV-R1, and then cloned into pGEM-T easy vector. The primer set sequences were HCV-F1: CTC CAG GTG AGA TCA ATA GG and HCV-R1: CGT GAC TAG GGC TAA GAT GG. RNA was synthesized using T7 and SP6 RNA polymerases. Template DNA was digested by DNase I, and RNA was purified using TRIZOL (Invitrogen) according to manufacturer's instructions.

RNAi

Knockdown of DDX3 was carried out using siRNA, DDX3 siRNA-1: 5′-GAU UCG UAG AAU AGU CGA ACA-3′, siRNA-2: 5′-GGA GUG AUU ACG AUG GCA UUG-3′, siRNA-3: 5′-GCC UCA GAU UCG UAG AAU AGU-3′ and control siRNA: 5′-GGG AAG AUC GGG UUA GAC UUC-3′. 20 pmol of each siRNA was transfected into HEK293 cells in 24-well plate with Lipofectamin 2000 according to manufacture's protocol. Knockdown of DDX3 was confirmed 48 hrs after siRNA transfection. Experiments were repeated twice for confirmation of the results.

Reporter assay

HEK293 cells (4×10^4 cells/well) cultured in 24-well plates were transfected with the expression vectors for IPS-1, DDX3 or empty vector together with the reporter plasmid (100 ng/well) and an internal control vector, phRL-TK (Promega) (2.5 ng/well) using FuGENE (Roche) as described previously [23]. The p-125 luc reporter containing the human IFN-beta promoter region (−125 to +19) was provided by Dr. T. Taniguchi (University of Tokyo, Tokyo, Japan). The total amount of DNA (500 ng/well) was kept constant by adding empty vector. After 24 hrs, cells were lysed in lysis buffer (Promega), and the *Firefly* and *Renella* luciferase activities were determined using a dual-luciferase reporter assay kit (Promega). The *Firefly* luciferase activity was normalized by *Renella* luciferase activity and is expressed as the fold stimulation relative to the activity in vector-transfected cells. Experiments were performed three times in duplicate (otherwise indicated in the legends).

PolyI:C or polyU/UC stimulation

PolyI:C was purchased from GE Healthcare company, and solved in milliQ water. For polyI:C treatment, polyI:C was mixed with DEAE-dextran (0.5 mg/ml) (Sigma) in the culture medium, and the cell culture supernatant was replaced with the medium containing polyI:C and DEAE-dextran. Using DEAE-dextran, polyI:C is incorporated into the cytoplasm to activate RIG-I/MDA5.

HCV 3′ UTR poly U/UC region (PU/UC) RNA (0∼50 ng/well), which is synthesized *in vitro* by T7 RNA polymerase, transfected into HEK293 cells in 24-well plate by lipofectamin 2000 (Invitrogen) with other plasmids. Cells were allowed to stand for 24∼48 hrs and HCV RNA-enhancing activation of IFN-beta promoter was assessed by reporter assay.

Immunoprecipitation (i.p.)

HEK293FT cells were transfected in a 6-well plate with plasmids encoding DDX3, IPS-1, RIG-I or MDA5 as indicated in the figures. 24 hrs after tranfection, the total cell lysate was prepared by lysis buffer (20 mM Tris-HCl [pH 7.5] containing 125 mM NaCl, 1 mM EDTA, 10% Glycerol, 1% NP-40, 30 mM NaF, 5 mM Na_3Vo_4, 20 mM IAA and 2 mM PMSF), and the protein was immunoprecipitated with anti-HA polyclonal (SIGMA) or anti-FLAG M2 monoclonal Ab (SIGMA). The precipitated samples were resolved on SDS-PAGE, blotted onto a nitrocellulose sheet and stained with anti-HA (HA1.1) monoclonal (SIGMA), anti-HA polyclonal or anti-FLAG M2 monoclonal Ab.

Pull-down assay

The pull-down assay was performed according to the method described in Saito T et al. [24]. Briefly, the RNA used for the assay was purchased from JBioS, Co. Ltd (Saitama, Japan). The RNA sequences are (sense strand) AAA CUG AAA GGG AGA AGU GAA AGU G, (antisense strand)CAC UUU CAC UUC UCC CUU UCA GUU U. The biotin is conjugated at U residue at the 3′ end of antisence strand (underlined). Biotinylated double-stranded (ds)RNA were incubated for 1 hr at 25°C with 10 μg of protein from the cytoplasmic fraction of cells that were transfected with Flag-tagged RIG-I and HA-tagged DDX3 expressing vectors. The mixture was transferred into 400 μl of lysis buffer containing 25 μl of streptavidine Sepharose beads, rocked at 4°C for 2 h, collected by centrifugation, washed three times, resuspended in SDS sample buffer.

Proteome analysis of RNA-binding proteins

RNA-binding proteins were identified by affinity chromatography and Mass spectrometry. Briefly, cell lysate was prepared from human HEK293 or Raji cells as will be described elsewhere (Watanabe and Matsumoto, manuscript submitted for publication). The lysate was first applied to polyU-Sepharose and then the pass-through fraction was applied to PolyI:C-Sepharose. The eluted proteins were analyzed on Mass spectrometry using the MASCOT software.

Confocal analysis

HCV replicon-positive (O) or –negative (Oc) cells were plated onto cover glass in a 24-well plate. In the following day, cells were transfected with indicated plasmids using Fugene HD (Roch). The

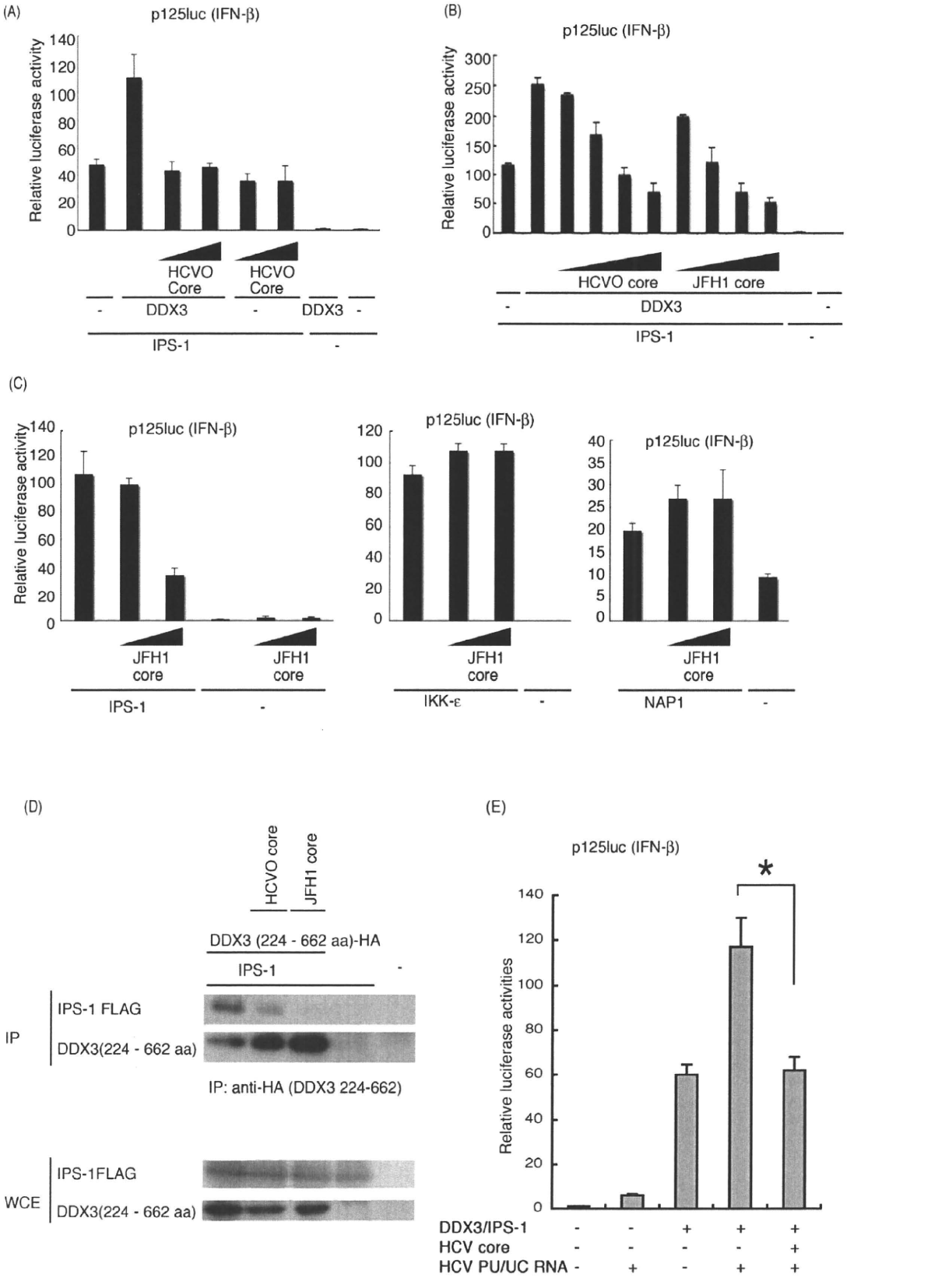
(A)
p125luc (IFN-β)
Relative luciferase activity
HCVO Core
HCVO Core
DDX3
DDX3
IPS-1
(B)
p125luc (IFN-β)
Relative luciferase activity
HCVO core
JFH1 core
DDX3
IPS-1
(C)
p125luc (IFN-β)
Relative luciferase activity
JFH1 core
JFH1 core
IPS-1
IKK-ε
NAP1
(D)
HCVO core
JFH1 core
DDX3 (224 - 662 aa)-HA
IPS-1
IP
IPS-1 FLAG
DDX3(224 - 662 aa)
IP: anti-HA (DDX3 224-662)
WCE
IPS-1FLAG
DDX3(224 - 662 aa)
(E)
p125luc (IFN-β)
Relative luciferase activities
DDX3/IPS-1
HCV core
HCV PU/UC RNA

Figure 4. HCV core protein inhibits DDX3 promotion of IPS-1-mediated IFN-beta induction. (A) Expression plasmids for IPS-1 (100 ng), DDX3 (200 ng) and/or HCVO core (50 or 100 ng) were transfected into HEK293 cells in 24-well plates with reporter plasmids, and reporter activity was examined. (B) Expression plasmids for IPS-1 (100 ng), DDX3 (100 ng), and/or HCVO or JFH1 core (10, 25, 50 or 100 ng) were transfected into HEK293 cells, and reporter gene expression was analyzed. (C) IPS-1-, IKKepsilon- or NAP1-expressing plasmids were transfected into HEK293 cells with HCV JFH1 core-expressing plasmids (25 or 100 ng), for reporter gene analysis. (D) Plasmids for expression of FLAG-tagged IPS-1 (400 ng), HA-tagged DDX3 partial fragment (400 ng) and HCVO or JFH1 core (400 ng) were transfected into HEK293FT cells. 24 hrs later cells were lyzed and the lysate was incubated with anti-HA Ab for immunoprecipitation. The DDX3 (224-662)-bound IPS-1 was blotted onto a sheet and probed with anti-Flag Ab. Whole cell lysate was also stained with anti-tag Abs. (E) IPS-1 (100 ng), DDX3 (100 ng), JFH1 core (50 ng) and/or p125 luc reporter (100 ng) plasmids were transfected with HEK293 cells, with HCV 3′UTR poly-U/UC (PU/UC) RNA (25 ng), synthesized *in vitro*. Cell lysates were prepared after 24 hrs, and luciferase activities measured. One representative of at least three independent experiments is shown except for panel D, which is a representative of two sets of the experiments.
doi:10.1371/journal.pone.0014258.g004

amount of DNA was kept constant by adding empty vector. After 24 hrs, cells were fixed with 3% of paraformaldehyde in PBS for 30 minutes, and then permeabilized with PBS containing 0.2% of Triton X-100 for 15 min. Permeabilized cells were blocked with PBS containing 1% BSA, and were labeled with anti-Flag M2 mAb (Sigma) or anti-HA pAb (Sigma) in 1% BSA/PBS for 1 hr at room temperature [25]. In some cases, endogenous proteins were directly stained with anti-core (C7-50) mAb (Affinity BioReagents, Inc) or anti-DDX3 pAbs (Abcam, Cambridge MA). The cells were then washed with 1% BSA/PBS and treated for 30 min at room temperature with Alexa-conjugated antibodies (Molecular Probes). Thereafter, micro-cover glass was mounted onto slide glass using PBS containing 2.3% DABCO and 50% of glycerol. The stained cells were visualized at ×60 magnification under a FLUOVIEW (Olympus, Tokyo, Japan).

Results

DDX3 binds RNA species

We have performed proteome analyses of RNA-binding fractions in human dendritic cell lysate eluted from polyU and polyI:C Sepharose. 127 cytoplasmic proteins were reproducibly identified as polyI:C-binding proteins (Watanabe and Matsumoto, unpublished data). Four of them are DEAD/H box helicases. In this setting, we found DDX3 is a RNA-binding protein (Fig. 1A). DDX3 in cell lysate bound both polyU and polyI:C, while the control PKR bound only to polyI:C.

Using biotinylayed dsRNA, RNA-binding properties of DDX3 and RIG-I were tested by pull-down assay. DDX3 or RIG-I protein was co-precipitated with dsRNA in HEK293 cells expressing either alone of DDX3 or RIG-I (Fig. 1B). Strikingly, higher amounts of DDX3 and RIG-I were precipitated with dsRNA in cells expressing both proteins (Fig. 1B). This, taken together with previous results [11,14,16], indicates that DDX3 assembles in some RNA, RIG-I, IPS-1 and HCV core protein in its C-terminal domain (Fig. S1).

PolyU/UC but not replicon enhances IFN-β induction via IPS-1/DDX3

A polyU/UC sequence is present in the 3′-region of the HCV genome, and serves as a ligand for RIG-I in IPS-1 pathway activation [23]. We produced the polyU/UC RNA and tested its IFN-beta-inducing activity in the presence or absence of DDX3 and IPS-1 (Fig. 2A). HCV polyU/UC promoted IPS-1-mediated IFN-beta induction, and this was further enhanced by forced expression of DDX3/IPS-1 (Fig. 2A). Similar results were obtained with wild-type mouse embryonic fibroblasts (MEF) (Fig. 2B). We also investigated whether DDX3 enhanced IPS-1-mediated IFN-β promoter activation in a RIG-I −/− MEF background (Fig. 2B). In IPS-1/DDX3-expressing MEF cells, polyU/UC IFN-induction was almost totally abrogated by the lack of RIG-I, suggesting that the trace RIG-I protein in the IPS-1 complex is required for DDX3 enhancement of the polyU/UC-mediated IFN response.

DDX3 mRNA (Fig. 2C) and protein [11] were depleted in HEK293 cells by gene silencing with si-1 siRNA, so this was used for DDX3 loss-of-function analysis. Control or DDX3-silinced cells were transfected with increasing amounts of polyU/UC and IFN-beta promoter activation was determined by luciferase assay. DDX3 loss-of-function resulted in a decrease of promoter activation by intrinsic polyU/UC (Fig. 2D). The result was confirmed with cells over-expressing RIG-I and exogenous polyI:C stimulation. HEK293 cells were transfected with a plasmid for the expression of RIG-I and stimulated with polyI:C, an activator of the IPS-1 pathway (Fig. S2A). IFN-beta reporter activation was suppressed in si-1-treated cells that expressed RIG-I, since polyI:C lots often contain short size duplexes that can activate RIG-I [26]. In addition, DDX3 augmented the IFN-beta response in cells expressing MDA5/IPS-1 (Fig. S2B). Thus, DDX3 was also crucial for IPS-1-mediated IFN-beta promoter activation.

We next determined whether the HCV replicon triggers IPS-1/DDX3 IFN promoter activation, using human hepatocyte lines with the HCV replicon (O cells) or without it (Oc cells). In O cells with the HCV replicon, IPS-1/DDX3 expression showed minimal enhancement of IFN-beta promoter activation (Fig. 3A), while in control Oc cells with no replicon, DDX3 facilitated IFN-beta promoter activation (Fig. 3B). Similarily, an augmented IFN promoter response to polyU/UC was observed in control Oc cells, but not in O cells (Figs. 3C and 3D). HCV RNA was prepared from O cells, and its ability to activate the IFN-beta reporter was tested in HEK293 cells (Fig. 3E). The HCV RNA of O cells had a high potency to induce reporter activation, and this activity was largely abrogated by si-1 siRNA treatment. Therefore, DDX3 augments IPS-1-mediated IFN-beta promoter activation in hepatocyte O cells, and HCV RNA, presumably the 3′UTR, participates in this induction. However, no IFN-beta reporter activation was detected in O cells which harbor HCV replicon. Therefore, an unidentified viral factor appeared to participate in suppressing virus RNA-mediated IFN-beta induction, which occurred in O cells overexpressing DDX3/IPS-1.

HCV core protein inhibits IPS-1 signaling through DDX3

What HCV proteins participate in IFN-beta induction was tested in a pilot study using protein expression analysis. We found that expression of HCV core protein as well as NS3/4A led to suppression of IFN-beta reporter activity in Oc cells (data not shown). The HCV core protein physically binds DDX3 [14,16], and co-localizes with DDX3 in the cytoplasm of HeLa cells transfected with HCV core protein [14]. Furthermore, we showed that DDX3 binds IPS-1, which resides on the mitochondrial outer membrane, and assembles into RNA-sensing receptors. Since some populations of the HCV core protein localize on the mitochondrial outer membrane [27], we tested if HCV core

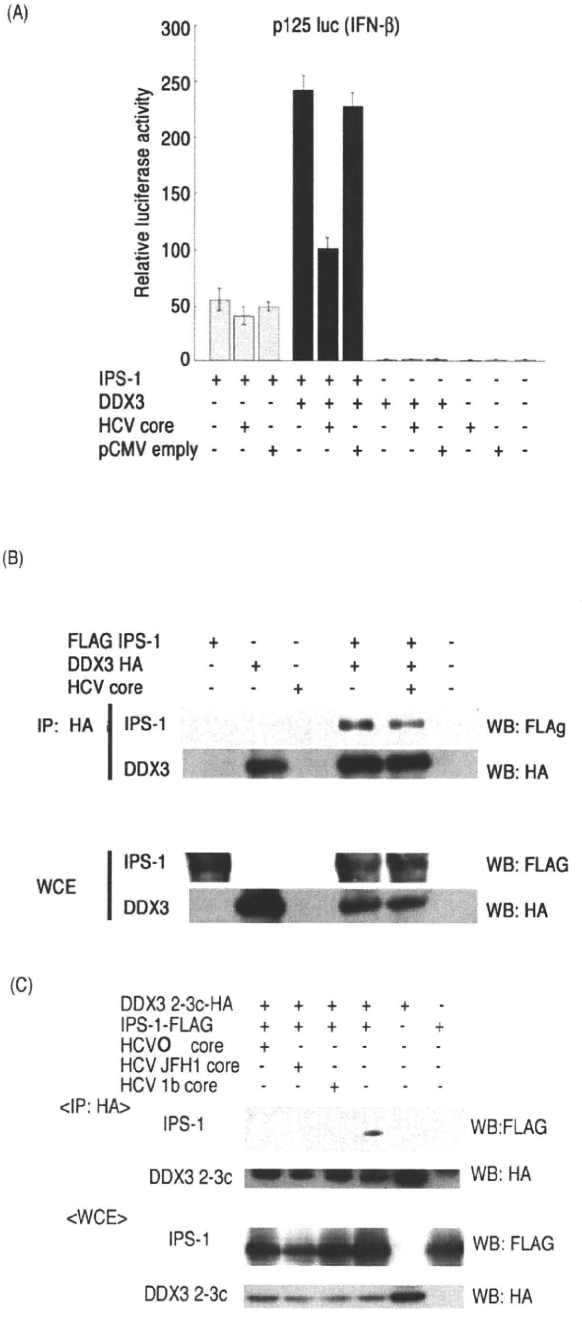

Figure 5. Properties of a 1b-type core protein in the IPS-1 pathway. (A) A core protein derived from an HCV patient suppressed DDX3-mediated activation of IPS-1 signaling. The 1b-type core protein was cloned into the pCMV vector from a patient with hepatitis C. IPS-1 (100 ng), DDX3 (100 ng) and HCV core (100 ng) expression vectors were transfected into HEK293 cells with a reporter plasmid (p125luc), for analysis as in Figure 4. (B) The core protein reduced interaction between full-length DDX3 and IPS-1. The plasmids encoding core protein (400 ng), DDX3-HA (400 ng) and FLAG-IPS-1 (400 ng) were transfected into HEK293FT cells. After 24 hrs, cell lysates were prepared and immunoprecipitation was carried out using anti-HA (DDX3-HA). (C) The core protein blocked interaction between the C-terminal fragment of DDX3 and IPS-1. The C-terminal region of DDX3 (199–662 aa) called DDX3 2-3c, IPS-1, HCV (O) and JFH1 or 1b core expression plasmids were transfected into HEK293FT cells. After 24 hrs, cell lysates were prepared and immunoprecipitation was carried out with anti-HA (DDX3 2–3c). Immunoprecipitates were analyzed by SDS-PAGE and Western blotting with anti-HA or FLAG antibodies. The results are representative of two independent experiments.
doi:10.1371/journal.pone.0014258.g005

protein affects IPS-1 signaling by binding to DDX3. The cDNAs for HCV core proteins, genotype 1b (HCVO) and 2a (JFH1) [16], were co-transfected into HEK293 together with IPS-1, DDX3, and reporter plasmids, and core protein interference with IPS-1/DDX3-mediated IFN-beta promoter activation was examined. We found that the core proteins of HCVO and JFH1 suppressed IPS-1/DDX3-augmented IFN-beta-induction in a dose-dependent manner (Fig. 4A and 4B). Without DDX3 transfection, core protein had no effect on IPS-1-mediated IFN-beta promoter activation (Fig. 4A). JFH1 core slightly more efficiently inhibited IPS-1/DDX3-augmented IFN-beta-induction than HCVO core (Fig. 4B).

Although some endogenous DDX3 was present in the cytoplasm without DDX3 transfection, only IPS-1 transfection permitted minimal induction of IFN-beta. It is notable that high doses of the HCV JFH1 core protein was needed to inhibit the IPS-1-mediated IFN-beta-induction signal (Fig. 4C, left panel). Since the imaging profile of DDX3 is not always monotonous in human cells, its distribution may be biased in the cytoplasm, which may reason that only a high dose of HCV core involves preoccupied DDX3 protein to inhibit the IPS-1 pathway. This is consistent with earlier reports on an NS3-independent mechanism to block IFN induction using HCV-infected Huh 7 cells [28].

IPS-1 transduces a RNA replication signal to result in IFN-beta output using downstream proteins, such as NAP1 and IKKeysilon. If the HCV core protein interferes with IPS-1 function through DDX3, the core should not inhibit over-expressed downstream molecules. As predicted, HCV core protein did not suppress the IKKepsilon- or NAP1-mediated IFN-beta-inducing signal (Fig. 4C, center and right panels). Hence, the core protein blocks the action of endogenous DDX3 and overexpressed IPS-1 to facilitate minimal IFN-beta promoter activation, and this IFN-beta blocking function of core does not target IKKepsilon or NAP1 (Fig. 4C). An upstream molecule of IKKepsilon and NAP1 is predicted to be the target of the HCV core protein, which is in line with the fact that the HCV core protein interacts with DDX3 [14,16].

To further confirm this model, we examined whether the HCV core protein inhibits the physical interaction between IPS-1 and DDX3. Full length IPS-1 and the C-terminal fragment of DDX3, which binds to the IPS-1 CARD-like region, were transfected into HEK293 cells, with or without the HCV core protein, and the DDX3 fragment was immunoprecipitated. Expression of HCV core proteins strongly inhibited interaction between the DDX3 C-terminal fragment and IPS-1 (Fig. 4D). JFH1 core appeared to show greater inhibition to DDX3-IPS-1 interaction than HCVO. We then examined this IFN-beta blocking function of JFH1 core in a similar cell condition plus polyU/UC. DDX3/IPS-1-enhanced p125luc reporter activity in cells stimulated with polyU/UC (Fig. 4E) was decreased in cells expressing HCV core. The results suggest that the role of the core in HCV-infected cells is to remove DDX3 from IPS-1, and facilitate its interaction with HCV replication complex (Fig. S1).

PolyU/UC HCV RNA activates the IFN-beta promoter (Fig. 2A), and this activity was inhibited by expression of the HCV core protein (Fig. 4E). PolyI:C/RIG-I-mediated IFN-β promoter activation was similarly suppressed by the core protein

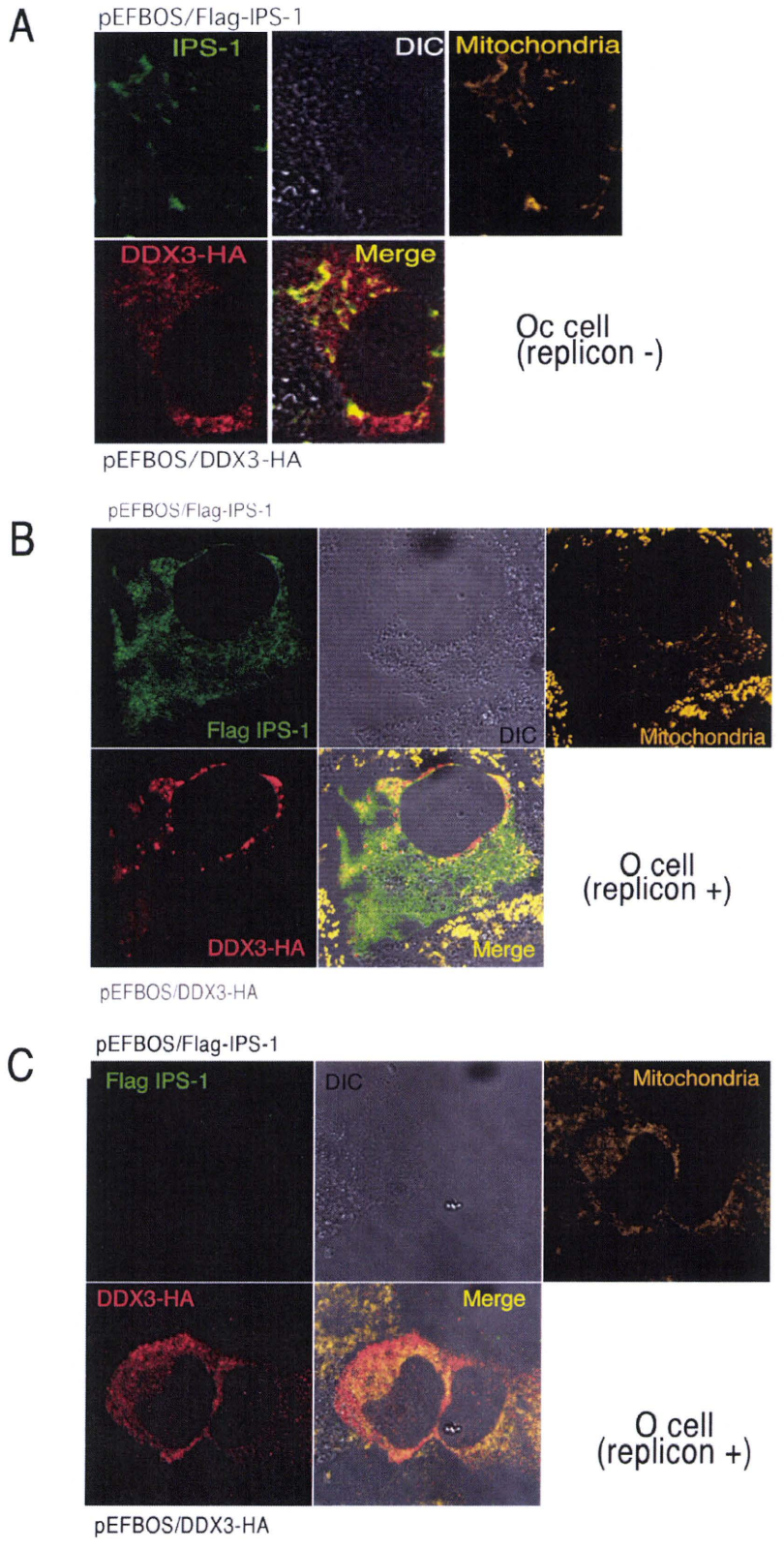
A
pEFBOS/Flag-IPS-1
IPS-1
DIC
Mitochondria
DDX3-HA
Merge
Oc cell
(replicon -)
pEFBOS/DDX3-HA
B
pEFBOS/Flag-IPS-1
Flag IPS-1
DIC
Mitochondria
DDX3-HA
Merge
O cell
(replicon +)
pEFBOS/DDX3-HA
C
pEFBOS/Flag-IPS-1
Flag IPS-1
DIC
Mitochondria
DDX3-HA
Merge
O cell
(replicon +)
pEFBOS/DDX3-HA

Figure 6. Distribution of DDX3 and IPS-1. (A) DDX3 colocalizes with IPS-1 on the mitochondria in Oc cells. HA-tagged DDX3 and FLAG-tagged IPS-1 were co-transfected into Oc cells. After 24 hrs, cells were fixed with formaldehyde and stained with anti-HA polyclonal and FLAG monoclonal Abs. Alexa488 (DDX3-HA) or Alexa633 antibody was used for second antibody. Mitochondria were stained with Mitotracker Red. Similar IPS-1-DDX3 merging profiles were observed in Huh7.5.1 cells (Fig. S3). (B,C) O cells with the HCV replicon poorly formed the DDX3-IPS-1 complex. Plasmids carrying IPS-1 (100 ng) or DDX3 (150 or 300 ng) were transfected into O (HCV replicon +) as in Oc cells (no replicon, panel A). After 24 hrs, localization of IPS-1 and DDX3 was examined by confocal microscopy. Two representatives which differ from the conventional profile (as in panel A) are shown. Similar sets of experiments were performed four times to confirm the results.
doi:10.1371/journal.pone.0014258.g006

(Fig. S2A). MDA5-dependent IFN-beta promoter activation was also suppressed by the core expression (Fig. S2B). The inhibitory effect of the core protein on DDX3-IPS-1 interaction was further confirmed using an 1b core isoform isolated from a patient. This HCV core protein also reduced interaction as well as IPS-1-mediated IFN-beta promoter activation (Fig. 5A). The blocking effect was relatively weak in cells expressing IPS-1 and full-length DDX3 (Fig. 5B). We presume that this is because there are multiple binding sites for IPS-1 in the DDX3 whole molecule [11]. For binding assay, we used DDX3 2-3c (across a.a. 199~662, longer than 224~662) instead of the whole DDX3. In fact, DDX3(199-662)-IPS-1 interaction was blocked by the additional expression of core protein (HCVO, JFH1 or 1b core) in Fig. 5C. Ultimately, HCV core protein suppresses IPS-1 signaling by blocking the interaction between the C-terminal region of DDX3 and the CARD-like region of IPS-1, and this inhibition apparently causes the disruption of the active RIG-I/DDX3/IPS-1 complex that efficiently induces IFN-beta production signaling.

Localization of DDX3 and HCV core protein in O cells

We attempted to confirm this finding by tag-expressed proteins and imaging analysis. In Huh7.5 cells IPS-1 colocalized with DDX3 around the mitochondria (Fig. S3), and so did in the hepatocyte lines Oc cells with no HCV replicon (Fig. 6A). In Oc and Huh7.5.1 cells with no HCV replicon, abnormal distribution of IPS-1 was barely observed (Fig. 6A, Fig. S3). In O cells expressing DDX3 and IPS-1, by contrast, two distinct profiles of IPS-1 were observed in addition to the Fig. 6A pattern of IPS-1: diminution or spreading of the IPS-1 protein over mitochondria (Fig. 6B,C). IPS-1 may be degraded by NS3/4A in some replicon-expressing O cells as reported previously [5,28]. We counted number of cells having the pattern represented by Fig. 6 panel B and those similar to Fig. 6 panel C, and in most cases the latter patterns were predominant.

What happens in the O cells with replicon when the core protein is expressed was next tested. Using O and Oc cells, we tested the localization of the core protein and DDX3 in comparison with IFN-inducing properties (Fig. 3). In O cells with full-length HCV replicon, DDX3 was localized proximal to the lipid droplets (LD) (Fig. 7A top panel) around which HCV particles assembled [29]. HCV core protein and DDX3 were partly colocalized in the HCV replicon-expressing cells (Fig. 7A center panel). The results were confirmed with HCV replicon-expressing O cells where endogenous core and DDX3 were stained (Fig. 7B upper panel). Partial merging between core and DDX3 was reproduced in this case, too. In contrast, sO cells, which possess a subgenomic replicon lacking the cording region of the core protein, showed no merging profile of DDX3 and LD (Fig. 7A bottom panel). Likewise, Oc cells barely formed assembly consisting of LD (where the core assembles) and overexpressed DDX3 (Fig. 7A bottom panel) or endogenous DDX3 (Fig. 7B lower panel). O cells expressing DDX3 tended to form large spots compared to Oc cells (with no replicon) and sO cells (core-less replicon) with DDX3.

Overexpressed DDX3 allowed the Oc cells to induce IPS-1-mediated IFN-beta promoter activation (Fig. 3B), while this failed to happen in O cells having HCV replicon (Fig. 3A). Ultimately, overexpressed IPS-1 did not facilitate efficient merging with DDX3 in O cells with replicon (Fig. 6B,C) compared to Oc cells or Huh7.5 cells with no replicon (Fig. 6A, Fig. S3). The results on the functional and immnoprecipitation analyses, together with the imaging profiles, infer that the IPS-1-enhancing function of DDX3 should be blocked by both NS3/4A-mediated IPS-1 degradation and the HCV core which translocates DDX3 from the IPS-1 complex to the proximity of LD in HCV replicon-expressing cells.

Discussion

We investigated the effect of the HCV core protein on the cytosolic DDX3 that forms a complex with IPS-1 to enhance the RIG-I-mediated RNA-sensing pathway. We demonstrated that the core protein removes DDX3 from the IFN-β-inducing complex, leading to suppression of IFN-β induction. DDX3 is functionally complex, since its protective role against viruses may be modulated by the synthesis of viral proteins. DDX3 acts on multiple steps in the IFN-inducing pathway [30]. In addition, DDX3 interacts with the HCV core protein in HCV-infected cells and promotes viral replication [16]. This alternative function is accelerated by the HCV core protein, resulting in augmented HCV propagation [14,16]. More recently, Patal et al., reported that interaction of DDX3 with core protein is not critical for the support of viral replication by DDX3, although DDX3 and core protein colocalize with lipid droplet [15]. If this is the case, what function is revealed by the interaction between DDX3 and HCV core protein remain unsettled. At least, HCV replication is not blocked by this molecular interaction [15].

It remains unclear in Fig. 4C why higher doses of JFH1 core protein are required to inhibit enhancement of IPS-1 signaling by endogenous DDX3 than by exogenously overexpressed DDX3. One possibility is that endogenous DDX3 is preoccupied in a molecular complex other than the IPS-1 pathway since DDX3 is involved in almost every step of RNA metabolism and its localization affects its functional profile [18,30].

Together with these findings, the results presented here suggest that the HCV core inactivates IPS-1 in a mode different from NS3/4A [5,31]. The core protein may switch DDX3 from an antiviral mode to an HCV propagation mode. The core protein localizes to the N-terminus of the HCV translation product, and is generated in infected cells before NS3/4A proteolytically liberates non-structural proteins and inactivates IPS-1. Our results on how the HCV core protein interferes with the interaction between DDX3 and IPS-1 add several possibilities to notions about the HCV function on the IFN-beta-inducing pathway [18].

DDX3 appears to be a prime target for viral manipulation, since at least three different viruses, including HCV [14], Hepatitis B virus [32], and poxviruses [8], encode proteins that interact with DDX3 and modulate its function. These viruses seem to co-opt DDX3, and also require it for replication. The viruses are all oncogenic, and may confer oncogenic properties to DDX3.